AN ANALYTICAL MODEL OF SURFACE WATER/GROUNDWATER INTERACTIONS IN A WESTERN WATERSHED EXPERIENCING CHANGES TO WATER AND LAND USE

By

Kimberly Peterson

HUMBOLDT STATE UNIVERSITY

A Thesis

Presented to

The Faculty of Humboldt State University

In Partial Fulfillment

Of the Requirements for the Degree

Master of Science

In Environmental Systems: Mathematical Modeling

August, 2011

AN ANALYTICAL MODEL OF SURFACE WATER/GROUNDWATER INTERACTIONS IN A WESTERN WATERSHED EXPERIENCING CHANGES TO WATER AND LAND USE

HUMBOLDT STATE UNIVERSITY

By

Kimberly D. Peterson

Approved by the Master's Thesis Committee:

Dr. Robert Van Kirk, Major Professor Date

Dr. Brad Finney, Committee Member Date

Dr. Diane Johnson, Committee Member Date

Dr. Christopher Dugaw, Graduate Coordinator Date

Dr. Jená Burges, Vice Provost Date

ABSTRACT

An Analytical Model of Surface Water/Groundwater Interactions in a Western Watershed Experiencing Changes to Water and Land Use

Kimberly Peterson

Watersheds throughout the western U.S. are experiencing changes to traditional irrigation practices and land use, resulting in changes to surface and groundwater hydrology. Teton Valley, in eastern Idaho and western Wyoming, is typical of western alluvial-fill valleys bounded by mountain ranges, in this case the Teton Range to the east, the Big Hole Mountains to the west, and the Snake River Range to the south. The primary water supply is snowmelt from the Teton Range, which flows to the Teton River in six major tributaries. In the late 19th century, homesteaders began diverting water from these tributaries for irrigated agriculture, which has been the dominant land use for the last century. Prior to the 1970s, conveyance occurred in earthen canals, and application occurred via flooding and other direct methods. In the late 20th century, most surface application was converted to sprinkler application, although most conveyance still occurs in the earthen canals. I developed an analytical model to investigate surface flows in the tributaries, as well as groundwater recharge, under five water management scenarios: the natural system (no irrigation), historical flood irrigation, actual 1979-2008 irrigation practices, 90% of irrigated land using sprinkler application (current condition), and future potential replacement of earthen canals with pipelines. I found that surface flow through the tributaries was highest under the natural scenario, at 73% of total inflow, and lowest under the flood irrigation scenario at 46%. Under the three irrigation scenarios that use canal conveyance, 46% to 49% of the water diverted was recharged to the shallow aquifer. Irrigation efficiencies for these scenarios

averaged 45% to 48%. Irrigation greatly increased groundwater recharge compared to the natural state, altering the hydrologic regime of a system naturally dominated by surface runoff from snowmelt. Replacing the canal system with pipelines could shift the hydrologic regime closer to the natural state and increase the amount of water available for direct crop use by 80% but decrease groundwater recharge by about 45%. Regardless whether diverted water is used for agriculture or other uses associated with land development, I found that changes in the conveyance system, not in application methods, have the greatest potential effect on hydrologic regimes. Depending on the resources being considered, such as spring discharge diverted by downstream irrigators or surface flow for aquatic species, these effects could be positive or negative.

ACKNOWLEDGEMENTS

I would like to thank my family for being so loving and supportive throughout my academic career. I would have never made it so far without you all. Father, you have inspired me in so many ways. Mother, you lift my spirits everyday. I would also like to give appreciation to the friends that have helped me along the way. You picked me up when I was down and gave me the strength to continue moving forward when I thought I had none, in particular my office mates.

I especially owe Dr. Rob Van Kirk a huge debt of gratitude. You have provided me with so many wonderful opportunities I would not have otherwise had. From my undergraduate degree through this thesis, you have helped me more than anyone else. I am very thankful that you have been a major part of my life.

Special thanks to the U.S. Department of Agriculture: Cooperative State Research, Education and Extension Service for the grant 2008-51130-19555. This grant afforded me the opportunity to continue my education. I also thank the people at Fremont-Madison Irrigation District, Friends of the Teton River, and the Henry's Fork Foundation for providing insightful information, allowing us to utilize office space and equipment, and for help in the field. I also thank the individual canal companies that allowed us access to their canal systems for field measurements.

Brian Apple and Lora Liegel contributed many efforts toward this project. They provided me valuable information and helped in the field. Thank you two for three great years of research.

TABLE OF CONTENTS

LIST OF FIGURES

LIST OF TABLES

1. INTRODUCTION

Many watersheds throughout the western U.S. are experiencing changes to traditional irrigation practices and land use, resulting in changes to surface water and groundwater hydrology (Van Kirk, 2008). Conjunctive management of surface water and groundwater is needed due to limited water supply and changing demands (Boggs et al., 2010). This requires a comprehensive understanding of the effects that land and water use changes can have on surface water/groundwater interactions. Natural hydrologic regimes were first altered with European settlement and development of irrigation (Van Kirk, 2008; Fiege, 1999). Current water availability and management strategies are based on these hydrologic regimes. However, these already altered hydrologic regimes are undergoing additional transformation as modern irrigation practices are replacing previous systems and as demand for domestic and municipal water supplies increases.

The changes affecting these mountain-basin regions have implications not only for human water use but also for ecological processes. Anthropogenic alteration of hydrologic regimes can have profound effects upon aquatic and riparian ecosystems (Poff et al., 1997; Richter et al., 2003; Petts, 2009). The initial development of irrigation affected such ecosystems, but irrigation has been in place long enough that aquatic and riparian ecosystems have adjusted to these irrigation-influenced hydrologic regimes (Fiege, 1999). As land use and irrigation practices change, these ecosystems may undergo further evolution.

The upper Teton watershed, located in eastern Idaho and western Wyoming, is an ideal location to study the effects of water and land use changes on surface water/groundwater interactions. It is typical of alluvial-fill valleys in the western U.S. The primary water supply is snowmelt from the Teton Range, which flows to the Teton River in six major tributaries. In the late 19th century, homesteaders began diverting water from these tributaries for irri-

gated agriculture, which has been the dominant land use for the last century. Prior to the 1970s, conveyance occurred in earthen canals, and application occurred via flooding and other direct methods. In the late 20th century, most surface application was converted to sprinkler application, although most conveyance still occurs in the earthen canals (Van Kirk and Jenkins, 2005). In addition, Teton County has undergone rapid urbanization in recent years. It was the fourth fastest growing county in the nation between 2000 and 2007, during which time its population grew 39% (Friends of the Teton River, 2009). The hydrogeology of the watershed is conducive to analysis of the effects of changes in land and water use on surface water/groundwater interactions because surface water and groundwater are highly connected. The relatively small aquifer is highly conductive, with low storativity, and therefore responds quickly (months to years) to changes in recharge, in contrast to the regional Eastern Snake Plain Aquifer, where response times are on the order of decades to centuries (Boggs et al., 2010).

The goal of this thesis is to examine the effect of water management changes on hydrology in the upper Teton watershed. More specifically, I developed a model to estimate the water budget for the Teton Range tributaries and the irrigation systems supplied by them. This will be accomplished by modeling diversions, surface flow, stream channel seepage, canal seepage, irrigation application seepage, and crop evapotranspiration (ET) under five scenarios: the natural system (no irrigation), flood irrigation (as practiced prior to the 1970s), actual 1979-2008 conditions, sprinkler irrigation, and potential replacement of earthen canals with pipelines (100% irrigation efficiency). This last scenario assumes that water is diverted to irrigate crops and/or landscaping but that the conveyance and application system is 100% efficient. A major objective is to estimate total groundwater recharge under the different scenarios. These recharge estimates will be used as inputs to a larger groundwater model being developed as a part of the USDA-funded project of which this

thesis is a component.

Throughout this thesis, I have chosen to use Imperial units of measure because these units are used in practice by watershed stakeholders, water managers, and water users. My intention is to maximize the utility of this thesis to these groups of people. To further increase the utility of this work at fine spatial and temporal scales, I have presented far more graphical and tabular information than is customary for a scientific paper. However, I have attempted to make the document as readable as possible by placing the figures and tables at the back of the document. Additionally, a large amount of detail in methodology was placed in appendices, to avoid letting details detract from larger objectives.

2. LITERATURE REVIEW

2.1. Study Area

A typical valley in the Intermountain West is formed by tectonic activity that causes mountain blocks to rise and basins to drop (Love et al., 2003). Streams erode the mountains, filling the valleys with alluvium. Fertile alluvial soil in these valleys allowed the establishment of agriculture beginning in the mid to late 19th century. These types of valleys are found in the Basin-Range Province and in the Rocky Mountains, including Teton Valley in eastern Idaho and western Wyoming.

2.1.1. Geology

The Teton watershed lies west of Grand Teton National Park and south of Yellowstone National Park. It is surrounded on the east by the Teton Range, on the south by the Snake River Range and on the west by the Big Hole Mountains. Elevations in the watershed range from about 12,000 feet at the peak of Teton Range to 5,800 feet at the northern boundary near Bitch Creek, and the valley itself is about 10 miles wide and 20 miles long (Figure 1).

The Sevier orogeny and the migration of the North American plate southwestward over the Yellowstone hotspot are the two major geologic events forming the Big Hole Mountains, the Snake River Range, and the Teton Range. The Big Hole Mountains and the Snake River Range were formed during the Sevier orogeny, which ended about 50 million years ago (Love et al., 2003). Five million years ago when the Yellowstone hotspot was at its closest proximity to what is now Teton Valley, the Teton Range started to form as a result of uplift that began along a normal fault located on the eastern side of the range (Love et al., 2003).

Teton Valley is filled primarily with alluvium from the Teton Range. The location of the Teton River on the western side of the valley is a result of continued uplift of the Teton Range to the east of the valley and deposition of alluvium in well-defined alluvial fans at the base of the range (Figures 1 and 2). Alluvium ranges in thickness from tens of feet at the mountain flanks to several hundred feet near the river (Kilburn, 1964; Nicklin Earth and Water, Inc., 2003; Van Kirk and Jenkins, 2005; Figure 2). Finer sediments with lower hydraulic conductivity create a relatively impervious layer further westward toward the Teton River (Friends of the Teton River, 2009).

2.1.2. Climate and Hydrology

In Driggs, Idaho, located on the valley floor in the Teton watershed, the mean temperature in January is 19°F and the mean temperature in July is 64°F, with an average annual temperature of 40°F (Van Kirk and Benjamin, 2000; Kilburn, 1964). Mean annual precipitation on the valley floor is 16 inches and is distributed almost uniformly throughout the year, June and July being the wettest months. At higher elevations, precipitation averages 30 to 50 inches annually, 60% to 70% of which falls as snow (Van Kirk and Benjamin, 2000). This snowpack constitutes the majority of the watershed's water supply.

The six major tributaries to Teton River are Trail Creek, Fox Creek, Darby Creek, Teton Creek, South Leigh Creek and North Leigh Creek (Figure 1). A seventh creek in the area, Badger Creek, does not flow across alluvial fans in the same manner as the other six (Figure 1). These six tributaries provide substantially more inflow than streams on the west side of the valley (Nicklin Earth and Water, Inc., 2003). They are incised in deep canyons upstream of the alluvial fans. Because alluvium is highly permeable, streams lose a substantial amount of water to the alluvial aquifer as they flow across the fans. Stream

seepage and direct snowmelt on the valley floor were the primary sources of recharge to the alluvial aquifer prior to European settlement. The groundwater in the alluvial aquifer flows westward until it reaches the less conductive fine sediments, at which point it discharges in a series of springs east of Teton River and returns to the river as surface flow (Figure 1).

2.1.3. Irrigation History

Irrigation for agricultural use began with settlement of the western U.S. By the mid 20th century, irrigation became the dominant use of water in the West, accounting for over 90% of total water withdrawls in most watersheds (Van Kirk, 2008). In Teton Valley, the majority of irrigation water is supplied by diversions from the tributaries draining the Teton Range, although a small amount is pumped from the aquifer (Van Kirk and Jenkins, 2005). There are no storage reservoirs in the upper Teton watershed. Teton Dam, the only large dam on the Teton River, was completed in June 1976 but failed just after the reservoir was filled and was never rebuilt (Van Kirk and Jenkins, 2005). Irrigation water is conveyed through canal systems, all of which were originally built as unlined earthen ditches. The points of diversions are located at the tops of the alluvial fans near the canyon mouths, resulting in substantial canal seepage to the aquifer as the canals deliver water to irrigated fields on the alluvial fans (Figure 3). In Teton Valley, some canal systems have been converted to pipelines, thereby reducing recharge. In the late 1960s, a canal system that diverts water from Trail Creek was converted to a pressurized pipeline system. Similarly, some irrigation water from Fox Creek is now conveyed through pipelines. It should be noted, however, that some seepage does occur in these systems. The canals are not always placed in pipes at the points of diversions but further downstream. Therefore seepage can occur from the canals in the reach from the point of diversion to the beginning

of the pipeline system. Also the pipelines themselves can leak.

Historically, most irrigation water was applied to crops by flooding and other direct methods. This was accomplished by spreading water directly to the land through a series of lateral ditches and allowing the water to percolate through the soil. This irrigation technique added another source of recharge to the aquifer. Irrigation efficiencies, defined as

$$\frac{\text{volume of irrigation water beneficially used}}{\text{volume of irrigation water diverted}}$$

(Burt et al., 1997; Zalidis et al., 1997), under this practice are reported to range from 45% to 60% (Venn et al., 2004). Beginning in the early 1970s, most flood irrigation in Teton Valley was replaced with sprinkler systems, and most agricultural land is irrigated this way today (Nicklin Earth and Water, Inc., 2003). Sprinkler irrigation efficiencies reportedly range from 60% to 80% (Venn et al., 2004).

Land use changes in many parts of the west have changed traditional irrigation practices (Kendy and Bredehoeft, 2006). Teton Valley, for instance, underwent rapid urbanization from 2000 to 2007 (Friends of the Teton River, 2009). This resulted in approximately 14% of agricultural land being developed for other uses such as housing and resorts in Teton Valley (Liegel, 2011). Such conversions could lead to further changes in irrigation conveyance and application or even abandonment of irrigation altogether, hence reducing recharge to the aquifer by eliminating seepage from both conveyance and application.

2.2. Surface Water/Groundwater Interactions

2.2.1. Mathematics of Surface Water/Groundwater Interactions

The first systematic experiment analyzing the flow of water through a porous medium was conducted by Henry Darcy in the mid-nineteenth century (Fetter, 1994). The experiment led to what is now known as Darcy's Law for groundwater flow given by

$$\overrightarrow{q} = -K\nabla h, \tag{1}$$

where $\overrightarrow{q}$ is the water flux vector (specific discharge) $\left[\frac{L^3}{TL^2} = \frac{L}{T}\right]$, K is a hydraulic conductivity tensor $\left[\frac{L}{T}\right]$, h is hydraulic head $[L]$, and ∇ is the gradient operator $\left[\frac{1}{L}\right]$. Standard assumptions and approximations lead to the linear diffusion equation for groundwater flow

$$\frac{\partial u}{\partial t} = \frac{Kh_0}{S_y}\left[\frac{\partial^2 u}{\partial x^2} + \frac{\partial^2 u}{\partial y^2}\right] + \frac{F(x,y,t)}{S_y}, \tag{2}$$

where $u(x,y,t) = h(x,y,t) - h_0$ $[L]$, h_0 is mean saturated thickness $[L]$, S_y is specific yield and is dimensionless, F is recharge $\left[\frac{L}{T}\right]$, x and y are spatial components in two dimensions $[L]$, and t is time $[T]$. This flow model has a diffusion coefficient $\frac{Kh_0}{S_y}$, which is the mean hydraulic diffusivity $\left[\frac{L^2}{T}\right]$. Specific boundary and initial conditions accompany Equation (2). Details of the derivation of this model are provided in Appendix A. To determine flow across a vertical surface in the aquifer, Darcy's Law is again utilized to obtain

$$Q(t) = -\iint_{\Omega} K\nabla h \cdot \overrightarrow{n}\, d\Omega, \tag{3}$$

where $Q(t)$ is flow $\left[\frac{L^3}{T}\right]$ across an oriented surface Ω with outward normal vector $\overrightarrow{n}$. Under certain geologic conditions, Equation (3) describes aquifer discharge to the surface. An example is spring discharge when water is forced to the surface by an impervious layer as in the study area.

2.2.2. Surface Water/Groundwater Interactions in Irrigated Areas

Conveyance and application are the two primary mechanisms for aquifer recharge due to irrigation (Johnson et al., 1999). Conveyance recharge occurs due to seepage from canals (Contor, 2008), which can increase groundwater levels (Helmus et al., 2009). Application recharge occurs due to leaky sprinkler pipes, poor irrigation system maintenance, and water applied to crops in excess of evapotranspiration (Burt et al., 1997; Kendy and Bredehoeft, 2006; Liu et al., 2004). Irrigation recharge can increase salt loads in rivers (Knight et al., 2004) yet may create and maintain permanent wetland ecosystems down-gradient of irrigated areas (Fiege, 1999; Peck and Lovvorn, 2001; Peck et al., 2005).

Distinguishing between conveyance and application efficiencies can be somewhat difficult. For example, a lined canal with flood application may produce an efficiency similar to having an unlined canal and sprinkler application. Zalidis et al. (1997) found that efficiency of irrigation systems in Northern Greece was about 60% under flood irrigation and 80% under sprinkler irrigation. Numerous other studies have reported decreased groundwater levels as a result of increased efficiency (Johnson et al., 1999; Boggs et al., 2010; Miller et al., 2006; Kendy and Bredehoeft, 2006; Venn et al., 2004; Nicklin Earth and Water, Inc., 2003).

Traditionally, high irrigation efficiency has been desired because it decreases the amount of surface water diverted for crops. However, increasing irrigation efficiency decreases

groundwater levels in areas where groundwater is not transported out of the basin. In such areas, increased irrigation efficiency can have unintended consequences. For example, pumping groundwater becomes more costly because wells must be dug deeper. Likewise, some downstream water users depend on springs that occur as a direct result of recharge from up-gradient irrigation. Wetland ecosystems dependent on irrigation seepage can also be negatively impacted by increased irrigation efficiency.

3. METHODS

This chapter describes model development and analysis. Section 3.1 outlines the modeling framework, which includes a description of the recharge components needed for the larger groundwater model. This outlines the four main sources of groundwater recharge: stream channel seepage, direct precipitation, canal leakage, and irrigation application. The surface water model is then described. Section 3.2 describes the collection and synthesis of streamflow and diversion data over the modeling trame frame of water years 1979-2008. Section 3.3 describes the seepage models. Section 3.4 describes the irrigation conversions for the five scenarios, and Section 3.5 describes model analysis.

3.1. Modeling Framework

The larger project of which this thesis is a component develops a groundwater model for the Teton Watershed based on Equation (2). The model domain and boundary conditions are presented in Appendix A. Because Nicklin Earth and Water, Inc. (2003) has already estimated water table heights and hydraulic gradients in the Teton Valley aquifer under scenarios roughly equivalent to those proposed in this work, I focus on streamflow rather than on hydraulic head as a response variable. Streamflow is an important response variable because almost all irrigators in Teton Valley use surface flow for irrigation and many aquatic species rely on surface flow to complete their life cycles. There is only one streamflow gage in Teton Valley with a continuous record over the entire modeling time frame (Teton River above South Leigh Creek, U.S. Geological Survey station 13052200), and it thus serves as the only spatial location at which to compare streamflow regimes across the various modeling scenarios. Fortunately, this gage is located near the northern (downgradient) boundary of the model domain, above which the majority of aquifer discharge

has been returned to the river via spring discharge. Therefore, I need only calculate the total discharge from the aquifer at the gage and not the spatial distribution of this discharge along the north-south line of springs (Figure 1). This allows me to reduce the problem to one spatial dimension by averaging across the aquifer length L. As shown in Appendix A, in the one-dimensional model, the recharge function in Equation (2) is averaged over the domain length to obtain a new recharge function

$$C(x,t) = \frac{1}{L}\int_0^L F(x,y,t)dy. \tag{4}$$

which has units $\left[\frac{L}{T}\right]$. This section describes the four components of $C(x,t)$ and the relationship among the surface flow and groundwater flow components.

3.1.1. The Recharge Function

The four sources of recharge to the aquifer are streams, direct precipitation (the majority of which is snowmelt), irrigation conveyance systems, and irrigation application. Thus, the recharge function can be written as

$$C(x,t) = C_{stream}(x,t) + C_{precip}(x,t) + C_{convey}(x,t) + C_{app}(x,t), \tag{5}$$

where the subscripts on the recharge function correspond to the four previously mentioned sources, x is the spatial component $[L]$, and t is time $[T]$. Because the groundwater flow equation has been linearized as described in Appendix A, the principle of superposition applies, so I can solve a different version of Equation (2) separately for each component F and then calculate the discharge back to the river due to that particular component. Four aquifer discharge functions $Q(t)$ will be obtained, one for each recharge component, and

the total discharge from the aquifer due to all four recharge sources is then

$$Q_g(t) = Q_{g\_stream}(t) + Q_{g\_precip}(t) + Q_{g\_convey}(t) + Q_{g\_app}(t), \tag{6}$$

where $Q_{g\_\text{“component”}}$ represents groundwater discharge from the various recharge components. The six major tributaries of the Teton River recharge the aquifer via channel seepage between the point of diversions at the top of the alluvial fans and either the point of dessication of the stream channel or the point where springs emerge. Below the springs, the tributaries gain water from aquifer discharge before flowing into the Teton River (Figure 3). The surface flow in a given tributary at any point on the alluvial fan reach is the flow at the top of the alluvial fan minus the cumulative stream seepage. Under natural conditions, the flow at the top of the fans is inflow from the mountains. Under irrigation scenarios, the flow at the top of the alluvial fans is inflow from the mountains minus any surface diversions. Stream seepage is discussed in detail in Section 3.3.2.

Precipitation in the summer is in the form of rainfall and is consumed by evapotranspiration (ET) (Allen and Robison, 2009). The only direct aquifer recharge is due to snowmelt in the spring. In this model, it is assumed that this component does not vary over the scenarios because I am not modeling effects of climate, but rather effects of water use changes. Because the model is linear as described in Appendix A, superposition will allow me to use Equation (6) to calculate discharge due to precipitation recharge, given knowledge of the other components. Thus, this component does not need to be modeled explicitly.

The irrigation canals recharge the aquifer via seepage along the entire length of the conveyance system. The amount of water applied to the fields is equal to the amount diverted into the canal system minus conveyance seepage (and a very small amount consumed by ET). Seepage from application is calculated as the amount applied minus crop ET demand.

Details of conveyance and application seepage are given in Section 3.3.

3.1.2. Surface Water Model for the Teton Watershed

For any given scenario, the total discharge, $Q_{gage}(t)$, at the Teton River gage above South Leigh Creek is

$$Q_{gage}^{scenario}(t) = Q_{surface}^{scenario}(t) + Q_{g}^{scenario}(t) + Q_{allother}^{scenario}(t), \tag{7}$$

where $Q_{surface}^{scenario}(t)$ represents the modeled tributary surface flows for the given scenario, $Q_{g}^{scenario}(t)$ is given by Equation (6) for that scenario, and $Q_{allother}^{scenario}(t)$ is the contribution of all other, unknown, inputs to flow at the gage (Figure 3). For the actual (1979-2008) scenario, all of the terms in Equation (7) are known except $Q_{allother}^{scenario}$, so I can solve for this unknown term. It is assumed this term is the same for all scenarios, so if $Q_{surface}^{scenario}$ and $Q_{g}^{scenario}$ are modeled for a given scenario, I can then calculate $Q_{gage}^{scenario}$. Specifically, decomposing Q_{g}^{actual} into its four components given in Equation (6) and rearranging Equation (7) yields

$$\begin{aligned} Q_{gage}^{actual}(t) - Q_{surface}^{actual}(t) - Q_{g\_stream}^{actual}(t) - Q_{g\_convey}^{actual}(t) - Q_{g\_app}^{actual} \\ = Q_{g\_precip}^{actual}(t) + Q_{allother}^{actual}(t), \end{aligned} \tag{8}$$

where $Q_{gage}^{actual}(t)$ is known, the surface component of this will be modeled in Section 3.2.1., and the groundwater model will produce the stream, conveyance, and application terms in Section 3.3 (Figure 3). The precipitation and "all other" terms are unknown.

Then, for example, under natural conditions, the only aquifer recharge is from the trib-

utaries and precipitation so Equation (7) gives

$$Q_{gage}^{natural}(t) = Q_{surface}^{natural}(t) + Q_{g\_stream}^{natural}(t) + \left[Q_{g\_precip}^{natural}(t) + Q_{allother}^{natural}\right]. \tag{9}$$

Because it is assumed that aquifer recharge from precipitation is constant across scenarios, $Q_{g\_precip}^{natural}(t) = Q_{g\_precip}^{actual}(t)$. Similarly, I assume $Q_{allother}^{scenario}(t)$ is constant across all scenarios. Using these assumptions, and substituting Equation (8) into Equation (9), produces total modeled discharge at the South Leigh gage under natural conditions,

$$\begin{aligned} Q_{gage}^{natural}(t) &= Q_{surface}^{natural}(t) + Q_{g\_stream}^{natural}(t) + Q_{gage}^{actual}(t) \\ &-Q_{surface}^{actual}(t) - Q_{g\_stream}^{actual}(t) - Q_{g\_convey}^{actual}(t) - Q_{g\_app}^{actual}, \end{aligned} \tag{10}$$

where all terms on the right-hand side, defined previously, are either measured directly or modeled. Similar calculations hold for the other scenarios.

This thesis focuses on computing and analyzing the recharge functions $C_{stream}(x,t)$, $C_{convey}(x,t)$, and $C_{app}(x,t)$ from Equation (5) and the stream surface component $Q_{surface}^{scenario}(t)$ component in Equation (7) under the five scenarios. These components will be used as inputs in the larger modeling effort.

3.2. Compilation and Synthesis of Streamflow and Diversion Rates

This section outlines data collection and synthesis procedures used in this study. All available canal and stream data were gathered from U.S. Geological Survey (USGS, http://waterdata.usgs.gov/nwis), Idaho Department of Water Resources (IDWR, http://www.idwr.idaho.gov), and Friends of the Teton River (FTR).

3.2.1. Streamflow

The streamflow models were developed for the alluvial aquifer on the east side of the Teton River in Teton Valley (Figure 1), which interacts with the six major tributaries draining the Teton Range and with canals diverting water from those tributaries. The tributaries from the Big Hole Mountains were ignored because they lay in a precipitation shadow and contribute only a small fraction of the total flow of the Teton River. Also, there is very little alluvial surface area for aquifer recharge on the west side of the river because the river lies on the west side of the valley (Figure 1).

The goal of these streamflow models was to estimate typical hydrographs for each tributary in the model domain. These models were developed to produce rough hydrographs during the modeling time period and capture the overall trends in the hydrologic regimes. They should not be analyzed for a particular day in a water year, but rather reveal the timing and magnitude of surface flow.

It was necessary to have modeling-period streamflow data for all six major tributaries, yet useful data existed only for Teton Creek and Trail Creek and not during the modeling period. Therefore statistical models were developed to synthesize streamflow data for the model time frame. Approximately 20 miles northeast of Teton Creek, outside of the watershed, lay Pacific Creek. Its watershed is similar in weather patterns and geography to the Teton Valley tributaries. This allowed Pacific Creek to be used as a surrogate creek from which to predict flows in the Teton Valley creeks. Daily flow data are available for Pacific Creek, Teton Creek and Trail Creek for water years 1947 to 1952, which allowed fitting statistical relationships between flow in Pacific Creek and that in Teton and Trail creeks. This relationship was modeled separately for Teton and Trail creeks.

The statistical relationship between flow in Pacific Creek and Trail Creek was given by

$$\ln[Q_{Trail}(t)] = \alpha + \beta \ln[Q_{Pacific}(t)] + \tau_i + \gamma_i \ln[Q_{Pacific}(t)] + \eta(t), \tag{11}$$

where α is the constant term, β represents the mean slope of the regression, i is the day of the water year, τ_i is the adjusted intercept for day i of the water year, γ_i is the slope adjustment for day i of the water year, and $\eta(t)$ is a random, normally distributed error component. This type of model was chosen because streamflow can usually be expressed as a power law and because the error terms will not be normal otherwise. A similar model was used for Teton Creek.

Due to strong daily streamflow autocorrelation, an auto-regressive time series model was used to decompose the error component as

$$\eta(t) = \zeta_1 \epsilon(t-1) + \zeta_2 \epsilon(t-2) + \zeta_3 \epsilon(t-3) + \epsilon(t), \tag{12}$$

where ζ_1, ζ_2, and ζ_3 are coefficients on lagged error terms and $\epsilon(t)$ is a temporally independent, normally distributed random variable. Only three lagged error terms were used because the partial autocorrelations were not statistically significant beyond this.

This model was fit to all six years of available data (1947-1952). To make predictions for the missing years, a full time series of independent errors, $\epsilon(t)$, was randomly generated, and Equations (11) and (12) were used to calculate $\ln[Q_{Trail}(t)]$. This process was repeated 1000 times and averaged across the replications. This average was exponentiated to obtain $Q_{Trail}(t)$. A similar method was used for Teton Creek. Standard model validation procedures were used to estimate accuracy and bias in the statistical predictions of flow in Teton and Trail creeks based on flow in Pacific Creek (Appendix B). Modeling efficiency

at the daily scale was 88.74% for Teton Creek and 94.25% for Trail Creek which were sufficiently high for this study.

The other four major tributaries are similar in elevation, aspect, geology, morphology and climate to Teton Creek (Figure 1, Table 1) but lacking in any useful streamflow data. Thus, flow in these creeks was estimated by scaling the Teton Creek predictions. The total water supply over a watershed is determined by multiplying the drainage area by the precipitation, so the scaling factor is the ratio of the annual water supply in the particular stream to that in Teton Creek. For example,

$$Q_{Fox}(t) = \frac{FoxArea * Precip}{TetonArea * Precip} Q_{Teton}(t).$$

The tributary basin parameters used to determine these ratios are provided in Table 1. The streamflow values synthesized by these methods represents flow in the streams at the tops of the alluvial fans upstream of all diversions.

3.2.2. Irrigation Application Method Conversion

A descriptive statistical model was developed of the temporal conversion from surface application (flood and sub-irrigation) to sprinkler application. No detailed data on this conversion have been compiled for Teton Valley, but data based on examination of aerial photographs and satellite images have been published for other areas in southeastern Idaho (Contor, 2004). I assumed that the temporal patterns of irrigation application conversion in Teton Valley were similar and thus fit statistical models to Contor's (2004) data. In general, this temporal pattern is one in which no land was irrigated with sprinklers prior to the 1960s, and the fraction of land under sprinkler irrigation increased continuously over time to its current value of about 90%. Because this data set consisted of only six data points, I

used an information-theoretic approach rather than data exploration to determine the best descriptive model (Burnham and Anderson, 2002). The response variable was the fraction, $p(t)$, of irrigated agricultural land under sprinkler irrigation in a given year, t. The "best" descriptive model of conversion to sprinkler application methods is given in Appendix C (Figure 4). Adjusted R^2 for this model was 87.5%, and residual assumptions were met. This model was used in subsequent analyses to estimate fraction of land under sprinkler irrigation in a given year.

3.2.3. Diversion Rates

Irrigation diversion rates from Teton Valley streams have been measured periodically during most irrigation seasons by IDWR or its designated water measurement authority; since 2005, FTR has been the designated measurement authority. Diversion data were obtained for irrigation seasons 1979-2000 from IDWR. These data consisted of measurements of diversion rates at each point of diversion on each of the six model streams. Generally, these measurements were made every five to seven days throughout the irrigation season. Diversion rates were summed over all points of diversion on each stream to obtain a single total diversion rate for that stream. I then used piecewise-cubic polynomial interpolation to interpolate daily diversion rates for days between measurements, assuming that diversion was zero prior to April 15 and after October 31, the dates bounding the IDWR-designated irrigation season in Teton Valley. Diversion data were obtained for irrigation seasons 2005-2008 (except that no data were available for Darby Creek for 2005) directly from FTR and used the same interpolation method to generate estimates of daily diversion rates for each stream for these water years.

No diversion data were collected by any entity during irrigation seasons 2001-2004

(2001-2005 on Darby Creek), forcing me to use a different method for estimating diversion rates for these years. This method was implemented separately on each of the six streams. I first averaged the interpolated daily diversion rates on each day of the irrigation season over the 26 years for which data were available (25 years for Darby Creek). The resulting averaged, irrigation-season diversion hydrograph was then normalized to obtain a unit hydrograph, which was then multiplied by an estimate of the total volume of diversion over the entire season to obtain a dimensioned diversion hydrograph for that season. To estimate the total annual diversion volume, I first computed total annual diversion volume for each of the years for which data were available. I then performed linear regression of total annual diversion versus total water-year streamflow and fraction of sprinkler-irrigated land, the latter of which was calculated from the descriptive model described above. Total annual diversion depended positively and significantly on total water-year streamflow for all six streams ($P < 0.10$ for all streams). Total annual diversion depended negatively and significantly on fraction of land from flood to sprinkler irrigation for all streams other than Fox and Darby creeks ($P < 0.10$ for each of the remaining four streams) due to decreased diversion rates. Fraction of land under sprinkler irrigation was then removed as a predictor of annual diversion volume for Fox and Darby creeks, and the regressions for these streams were performed again using total water-year streamflow as the only predictor. Residual analysis verified that the resulting regression models met error assumptions. These regression models explained between 24% and 59% of interannual variability in annual diversion rates, depending on the stream. These regression models were then used to predict total annual diversion volume for irrigation seasons 2001-2004 (2001-2005 for Darby Creek), and these predicted annual volumes were multiplied by the unit diversion hydrograph to obtain diversion hydrographs for these years.

The final step in estimating daily diversion was to compare estimated daily diversion

from each stream with the estimated daily flow for that stream (Section 3.2.1.) and reduce estimated daily diversion to no more than the total streamflow, if necessary.

3.3. Seepage Models

3.3.1. Channel Loss Rates

In order to develop seepage models, it was necessary to calculate loss rates in two types of channels: earthen irrigation canals and stream channels on the alluvial fans. A larger, watershed-scale study required canal loss rates for canals in the Lower Henry's Fork watershed. Because the two areas are geologically different, the Henry's Fork canals were treated as a separate group, yielding a third channel type.

To calculate loss rates, I designated a reach of channel where there are few or no surface inputs or outputs. I then measured discharge, Q, at the upstream and downstream boundary of the reach. Wetted area was estimated using maps, satelite imagery and field measurements. Then the loss rate, $r\left[\frac{L^3}{T}\cdot\frac{1}{L^2}\right]$, was calculated as

$$r = \frac{Q_{bottom} - Q_{top}}{WettedArea}. \tag{13}$$

Flow data used in Equation (13) were obtained from a variety of sources. Many measurements were compiled from IDWR watermaster reports from the 1930s and 1940s. I measured most of the canal loss data in the field. A few miscellaneous measurements were obtained from FTR and from a pilot study performed prior to receiving the grant for this study. From this study, estimated mean loss rates were 2.655 ft/day for Henry's Fork canals, 3.663 ft/day for Teton Valley canals, and 3.397 ft/day for streams on the Teton Valley alluvial fans (Table 2). By comparison, Wytzes (1980) reported canal loss rates ranging from 2

to 3.5 ft/day for canals on the Rigby Fan, which includes some of the Lower Henry's Fork canals measured in the study.

3.3.2. Stream Channel Seepage

Stream channel loss was modeled by

$$\frac{dQ}{dx} = -rw(x), \tag{14}$$

where $Q(x)$ is the discharge $\left[\frac{L^3}{T}\right]$ at location x downstream from the top of the losing reach in the stream, r is the measured loss rate $\left[\frac{L}{T}\right]$, and $w(x)$ is the wetted width of the stream $[L]$. Statistical analysis showed that wetted width could be described as a power function of discharge, that is, $w(x) = \alpha Q(x)^\beta$ for some α and β. Then Equation (14) can be written as

$$\frac{dQ}{dx} = -r\alpha Q(x)^\beta, \tag{15}$$

with initial condition $Q(0) = Q_0$, the amount of discharge in the stream just below all diversions, but at the top of the losing reach. The particular Q_0 was calculated on a daily basis by subtracting diversion (Section 3.2.3.) from streamflow (Section 3.2.1.). The ordinary differential equation (15) was solved using separation of variables, giving

$$Q(x) = [Q_0^{1-\beta} - (1-\beta)r\alpha x]^{\frac{1}{1-\beta}}. \tag{16}$$

For each tributary, α and β were determined by linear regression of ln($w(x)$) versus ln($Q(x)$). Data for these regressions were obtained from field measurements made by FTR. Analysis of covariance showed that β did not differ significantly across tributaries ($F_{4,69}$ =

$0.422, P = 0.729$). The mean value of β was 0.132. The α values were significantly different across streams ($F_{4,73} = 9.805, P = 10^{-6}$) and ranged from 13.956 to 22.032.

For $\beta < 1$, Equation (16) predicts that no water remains in the channel downstream of the point $x = \dfrac{Q_0^{1-\beta}}{(1-\beta)r\alpha} \equiv d$, which was defined as the point of dessication. Letting v be the total length of the losing reach, Equations (15) and (16) yield total loss over the losing reach as $Q_0 - [Q_0^{1-\beta} - (1-\beta)r\alpha a]^{\frac{1}{1-\beta}}$ where $a = \min(d, v)$. The amount of surface flow remaining in the channel at the bottom of the reach is 0 if $d < v$ and $Q(v)$ otherwise. These calculations were applied to each stream on each day to calculate stream channel loss and the amount of surface flow remaining in the channel at the bottom of the alluvial fan reach.

Total loss $\left[\dfrac{L^3}{T}\right]$ from the stream reach is the sum of loss to direct evaporation from the stream surface, loss to ET by riparian vegetation, and seepage to groundwater. I calculated loss to direct evaporation by multiplying daily evaporation rate $\left[\dfrac{L}{T}\right]$ by the total surface area [L^2] of water in the channel. Field measurements of stream channel geometry indicated that channels on the alluvial fan reaches were very wide and shallow. Thus, the width of the water surface at a given cross section is approximately equal to the wetted width, $w(x)$, given by the power function described above. Then the total surface area of the losing stream reach is given by the product of this width and the wetted length, a, of the losing reach. Loss to riparian vegetation ET was calculated by multiplying daily ET rate by the total area of riparian vegetation along the length of the losing reach. All daily evaporation and ET rates were obtained from ET Idaho (Allen and Robison, 2009). I used values reported for Driggs, Idaho, which is located in the center of the study area. For riparian vegetation, I used the average ET for cottonwoods and willows, which are the two most common riparian species in the study area. To estimate the total area of riparian vegetation along the stream channels, 10 points on each stream were randomly selected, and I mea-

sured total linear extent of riparian vegetation perpendicular to the stream channel at each of these points using Google Earth's measurement tool, and corrected these measurement for bias (Appendix D). The product of the mean of these riparian widths and the length of wetted stream channel yielded the total area of riparian vegetation. Loss to channel surface evaporation was subtracted first from total loss. Riparian ET loss was subtracted from any remaining loss. Finally, the amount of total loss recharged to groundwater was taken to be any loss remaining after subtracting surface evaporation and riparian vegetation ET. This was forced to be zero if ever negative.

3.3.3. Canal Seepage

Methods for calculating canal seepage were similar to those for calculating stream channel seepage. Conveyance loss for each day of each irrigation season was calculated by multiplying the mean loss rate by the total wetted area of the canal systems served by a given stream. Field measurements indicated that canals in Teton Valley were also very wide and shallow, so the wetted perimeter of a canal cross section was very nearly equal to the water surface width. Furthermore, the wetted perimeter of a given canal cross section was nearly independent of canal flow, as long as at least some water was flowing though the canal. Thus, it was assumed that for every day in which water is diverted into the canal system, total wetted area was the product of a given canal system's mean width and total length. In order to account for changes that were made to canal systems as a result of conversion to more efficient irrigation systems, I used pre-1970s diversion records, maps, and aerial images to estimate "historic" canal lengths and areas to use in the flood-irrigation scenario. The procedure for estimating the widths of canals and of canal-side vegetation strips was similar to that described above (see Appendix D for details). I again subtracted

canal surface evaporation and canal-side vegetation ET from conveyance loss, in that order, and any remaining conveyance loss was assumed to recharge groundwater. Any remaining surface flow in the canal after accounting for evaporation, canal-side vegetation ET and groundwater seepage was assumed to be applied to crops.

3.3.4. Application Seepage

Seepage to groundwater from irrigation application was defined to be the daily amount of water applied to crops in excess of crop ET demand, if any. To determine crop ET demand, I used Google Earth images and topographic maps to estimate the total area of land that could be served by diversions from the six study streams. This area was estimated at 45,000 acres, which included former agricultural land that had been subdivided or otherwise developed since 1970. These lands accounted for about 14% of the potentially irrigable lands in the model domain and were included because in many such cases of land conversion, the same surface water that was used to irrigate agricultural crops or pasture is now used or potentially could be used to irrigate landscaping (Liegel, 2011). Crop distribution was estimated using values reported in the National Agricultural Statistics Service (NASS) database (http://quickstats.nass.usda.gov/). I averaged the reported, county-level crop distributions over the available period of record (1997-present for most crops but 1979-present for a few crop types) to obtain mean values for crop distributions for Teton County. I then adjusted these figures to account for differences between crop distribution in the study area and that in the county as a whole. My estimate of mean crop distribution in the study area was 25% alfalfa, 45% grain, 5% potatoes, and 25% pasture/lawn. Daily crop ET demand was then calculated by taking the product of crop type percentage, total area of land served by the canal systems, and the daily, growing-season, actual ET for that crop

type, where the latter was obtained from the ET Idaho database (Allen and Robison 2009).

The calculated crop ET demand was very insensitive to crop type distribution because daily, growing-season ET rates for alfalfa (two-three cuttings, as is typical in the study area), grain, and pasture/lawn were very similar (Allen and Robison, 2009). Similarity in ET rates also implies that the ET demand calculations were insensitive to the actual land area that has been converted from agricultural to non-agricultural uses in the study area, under the assumption that lawn and other landscaping on converted lands is or could be irrigated with the same surface supply that was applied to that land prior to conversion. Because it was beyond the scope of this study and the data available for the model time frame to estimate the particular land cover type present on any given parcel of land irrigated by any particular canal system, the crop distributions and acreages are means applied over the entire model domain to obtain total ET demand for the study area. Total crop ET demand calculated in this way was then apportioned among the six model streams in proportion to mean modeling-period diversion rate, under the assumption that the land irrigated by a particular stream is proportional to water availability on that stream.

My method of calculating seepage to groundwater from irrigation application assumes that any water applied to the ground in excess of crop ET demand is recharged to groundwater rather than lost to evaporation. This assumption could potentially overestimate the amount of excess application that is recharged to groundwater. However, I did not subtract growing-season precipitation from total demand because this amount is generally small, on the order of 10% to 20% of total demand, hence leading to a potential underestimation of application in excess of crop ET. Lastly, not all land that can be irrigated by a given canal system is irrigated in any one growing season because of crop rotation and other factors. Thus, estimates of crop ET demand are theoretical maxima that assume full application across the model domain. Crop ET demand may be overestimated due to the assumption

that all water available on a particular day for crop ET is used for crop ET, when in fact alfalfa, hay and pasture may not be irrigated every day of the irrigation season even if water is available.

3.4. Scenarios

Applying the methods described above produced estimates of all model components under the climatic and irrigation management conditions that were actually experienced during water years 1979-2008. This set of conditions constituted what was termed the "actual" modeling scenario. To simulate "natural" hydrologic conditions over these same water years, I used the same inflow from the six model streams but assumed that no water was diverted for irrigation, leaving stream channel seepage as the only modeled source of groundwater recharge. I then simulated three other irrigation management scenarios over this same set of water years: 1) "flood" application, 2) "sprinkler" (or current) application, and 3) "pipeline" conveyance with sprinkler application (Table 3). The flood application scenario was intended to simulate irrigation practices that were used prior to the 1960s (historic canal system, surface application), the sprinkler application scenario was intended to simulate current practices (current canal system, 90% of application done with sprinklers), and the pipeline scenario was intended to simulate a theoretical scenario in which irrigation is 100% efficient (no conveyance loss and no application in excess of crop ET).

Diversion rates for the three irrigation scenarios were based on the actual diversion rates estimated using the methods described in Section 3.2.3. Statistical analysis of the dependence of diversion on the fraction of irrigated land under sprinkler application showed that, on average after accounting for variability in supply across water years, diversion under the 90% sprinkler scenario was 0.862 times that actually observed over 1979-2008,

and diversion under the flood scenario was 1.107 times that actually observed over 1979-2008 period (Appendix E). These ratios represent the relative efficiency (sprinkler) and inefficiency (flood) of the irrigation practices as compared to application practices actually used during the study period. I applied these proportions to the actual diversion figures to obtain diversion rates for the sprinkler and flood scenarios. This was done because the only diversion data available were during the actual 1979-2008 period and a scale factor was needed to synthesize diversion data for the other irrigation scenarios. As a final step in computing diversion rates under the flood irrigation scenario, I limited diversion on any given day from any given stream to the smaller of the predicted diversion and streamflow to ensure that diversion rates would not exceed available supply.

To compute diversion under the pipeline scenario, it was assumed that daily diversion on a given stream was the minimum of daily crop ET, streamflow, and period-of-record maximum diversion for that stream. This models a scenario in which diversion is limited to daily crop ET or available streamflow, whichever is smaller, and does not exceed the total irrigation system capacity, which I took to be the maximum daily diversion rate recorded during the period of record.

Conveyance loss for the flood and sprinkler scenarios was calculated as described in section 3.3.3, using the historic canal configuration for the flood scenario and the current canal configuration for the sprinkler scenario (Table 4). Application seepage was calculated as described in section 3.3.4. Conveyance loss and application seepage for the pipeline scenario was assumed to be 0. Flow remaining in the stream channel under all five scenarios was calculated as described in section 3.3.2.

3.5. Analysis of Model Output Data

A mean modeling-period water budget for the model domain was calculated for each of the five operating scenarios. This gives the distribution of water supply (inflow from the tributaries) among water surface and riparian vegetation evapotranspiration, stream channel seepage, canal seepage, application seepage, crop ET, and surface flow. I constructed hydrographs of surface flow remaining in the stream channel at the point of spring emergence for each tributary under each scenario. These depict the amount of surface water remaining in the channel after accounting for diversions, seepage, and ET. Summary statistics were computed over the 30 water years and graphed over day of the water year to produce the hydrographs. The mean daily flow across the 30 water years was also calculated and depicted.

For each tributary, scenario, and water year, I counted the number of days that surface flow was continuously maintained from the tops of the alluvial fans to the point of spring emergence. For most tributaries and years, this represents the duration of the spring/summer time period over which fish can migrate between headwater areas and the Teton River. I used Analysis of Variance (ANOVA) to test for differences in mean duration of this across potential irrigation period scenarios.

The amount of water in a tributary on a particular day at any location below the point of diversion is also ecologically important. Discharge in the stream under each scenario was plotted against the length of the stream below the point of diversion. This was done by taking the mean discharge across the 30 years for the days May 1st, June 15th, August 1st, and September 15th. These dates were chosen because they capture changes occurring over the irrigation season and also encompass the time frame of cutthroat trout spawning and emergent fry migrations.

I computed total groundwater recharge from all components and all tributaries for each scenario and water year. ANOVA was used to test for the difference in mean groundwater recharge across the scenarios. To investigate the effects of year-to-year variability in water supply on both groundwater recharge and sensitivity of recharge to differences across scenarios, I used regression analysis to investigate the dependence of total groundwater recharge, and of standard deviation in recharge across the scenarios, on total water supply. To assess the effect of each irrigation scenario on the overall hydrologic regime of the stream-aquifer system, I analyzed the percent of net supply (total supply minus ET) that flowed through the model domain as groundwater. Analysis methods were the same as those used for total groundwater recharge.

For all ANOVA tests, I treated year as a blocking variable and removed its effect prior to testing for differences across scenarios. Because year served as the observational unit for the regression analyses, I tested residuals for autocorrelation to ensure that residuals were temporally independent. For all statistical tests, I verified that residuals were normally distributed and transformed variables when needed to meet this condition.

4. RESULTS

The largest single component of the water budget under any scenario was surface flow immediately upstream of spring emergence, ranging from 46% of supply under the flood irrigation scenario to 73% of supply under the natural scenario (Figure 5). The highest total surface flow volume through the alluvial fan reaches occurred under the natural scenario, at an annual mean of 180,000 acre-feet, and the lowest total surface flow occurred under the flood irrigation scenario, at an annual mean of 110,000 acre-feet. The total amount of water diverted annually under the flood, actual, sprinkler and pipeline irrigation scenarios averaged 87,000, 81,100, 72,900 and 62,100 acre-feet, respectively. The percent of water diverted that enters the aquifer via canal seepage averaged 48% under the flood irrigation scenario, 46% under the actual scenario, and 49% under the sprinkler irrigation scenario. Application seepage was very low under all irrigation scenarios. Irrigation efficiency, as defined by the volume of water beneficially used by crops divided by total diversion (see Section 2.1.3), averaged 45% under the flood scenario, 48% under the actual scenario, and 47% under the sprinkler scenario and was assumed to be 100% under the pipeline scenario. Riparian ET was less than 1% of inflow in all cases. Under the pipeline scenario, the amount of water diverted that was potentially used by crop ET averaged 62,100 acre-feet per year. Crop ET for the other three irrigation scenarios averaged 34,300 to 39,000 acre-feet per year and varied little across the scenarios (Figure 5).

Across all creeks, surface flow remaining at the point of spring emergence was highest under the natural condition and lowest under flood irrigation (Figures 6-11). Surface flow under the pipeline scenario was generally greater than that under any of the other irrigation scenarios. The largest variation across scenarios in flow remaining at the springs occurred later in the irrigation season, from July 1st to October 1st (Figures 6-11). The

mean number of days surface flow reached the point of spring emergence was highest under the natural scenario and lowest under the flood irrigation scenario. After accounting for variability across water years, the mean number of days surface flow reach spring emergence differed significantly across scenarios ($F_{33,116}$ statistics yielded P values less than 2×10^{-16} for all streams). In all cases in which ANOVA was performed, such as here, first-order auto-regressive coefficients on the error components were less than 0.3, and generally around 0.1, and not significantly different from 0, implying temporal independence. Pairwise comparison tests showed that these differences were significant between any two scenarios ($P < 0.05$), except occasionally between the flood and actual scenarios and between the actual and sprinkler scenarios (Figures 12-17). Surface flow through the alluvial fan reaches as a function of stream length was also highest under the natural scenario and generally lowest under the flood scenario. Again, surface flow across these alluvial fan reaches under the pipeline scenario was greater than that under the other irrigation scenarios (Figures 18-23).

After eliminating the effect of interannual variability, mean annual groundwater recharge differed significantly across scenarios ($F_{33,116} = 87.27, P < 2 \times 10^{-16}$, Figure 24). Total groundwater recharge was lowest under the pipeline scenario and highest under the flood irrigation scenario. Total groundwater recharge was more similar between the natural and pipeline scenarios than between either of these two scenarios and the other three irrigation scenarios. Under all scenarios, total groundwater recharge was an increasing function of water supply (Figure 25 top, Table 5). As measured by the standard deviation across scenarios, difference in total groundwater recharge across scenarios was also an increasing function of supply ($F_{1,28} = 35.47, P = 0.02$, Figure 25 bottom), indicating that the effect of irrigation scenario on groundwater recharge was smallest in the dry water years and largest in the wet years.

Upon removing interannual variability, the percent of the supply moving through the groundwater system differed across scenarios ($F_{33,116} = 159.9, P < 2.2 \times 10^{-16}$, Figure 26). The percent of net supply moving through the aquifer was lowest under the natural scenario at approximately 30% and highest under the flood scenario at approximately 50%. The pipeline scenario was more similar to the natural scenario than to the other three irrigation scenarios (Figure 26). Under all scenarios, the percent of net supply that moved through the aquifer was a decreasing function of total water supply (Figure 27 top, Table 6). Standard deviation in this percent across scenarios was also a decreasing function of total supply ($F_{1,28} = 28.30, P = 1.2 \times 10^{-6}$, Figure 27 bottom), indicating that the differences in overall hydrologic regime across scenarios were greatest in the dry years and smallest in the wet years.

5. DISCUSSION

Introduction of canal systems into Teton Valley changed surface and groundwater hydrology. Irrigation application and conveyance has resulted in more recharge to the alluvial aquifer than occurred under the natural system. The reason for this is that water is spread over a larger surface area, allowing for more seepage. Different irrigation scenarios have different effects on surface water and groundwater, but differences among the flood, actual and sprinkler scenarios were small because all of these use essentially the same conveyance system, losses from which dominated the water budget of diverted water. Surface flow through the model domain was highest under the natural condition because no water was diverted for crops. In contrast, surface flow was lowest under the flood irrigation scenario because more water was diverted. Surface flow under the pipeline scenario was greater than that under any of the other irrigation scenarios.

Irrigation efficiencies were low across all irrigation scenarios (except the pipeline scenario, which was assumed to be 100% efficient), ranging from 45% to 48%. Venn et al. (2004) found irrigation efficiencies ranging from 45% to 60% for flood irrigation and 60% to 80% for sprinkler irrigation. Zalidis et al. (1997) found similar results, with flood irrigation efficiency at approximately 60% and sprinkler irrigation efficiency at approximately 80%. The reason that Teton Valley irrigation efficiencies were comparatively low is because most loss was due to conveyance, which was essentially the same under the flood, actual and sprinkler scenarios. Furthermore, loss rates are very high in Teton Valley (over 3 ft/day), and the canal system has a large area (Table 4). Wytzes (1980) found similar loss rates on the Rigby Fan located in the lower Henry's Fork, but he reported canal seepage to be only about 35% of diversion. This lower percentage occurrs because the canals on the Rigby Fan are much larger and have a higher discharge to surface area ratio. I found that

irrigation efficiency was highest under the actual scenario (excluding the pipeline scenario, which was assumed to be 100% efficient). It was expected that sprinkler irrigation would be more efficient; however, more water was diverted under the actual scenario at times when it could be applied to crop ET, allowing more consumptive use by crops. Flood irrigation had the lowest irrigation efficiency because more water was lost to both conveyance and application seepage. Small differences in the efficiencies among these three scenarios could be due in part to assumptions that were made about the temporal aspects of conversion from flood to sprinkler irrigation.

Because most seepage occurs in the conveyance system, application seepage is very low. By the time water that has not seeped into the aquifer has made it to the crops, there is just enough or not even enough, to meet demand. Because application seepage is low, the largest changes to hydrologic regimes are related to changes in the conveyance system, and not changes in application methods. Nicklin Earth and Water, Inc. (2003) obtained similar results from his groundwater model. Although conversion from flood to sprinkler irrigation resulted in reductions in groundwater levels in Teton Valley, these reductions were small, ranging from 0 to 8 feet out of a saturated thickness of several hundred feet (Nicklin Earth and Water, Inc., 2003).

Consumptive use of diverted water was highest by volume under the pipeline scenario, even though this scenario resulted in the least amount of diversion. Because the pipeline scenario was 100% efficient, all of the diverted water reached crops, allowing an increased amount to be used by crop ET, even at lower rates of diversion. Increased efficiency under the pipeline scenario could increase the volume of water available for direct use by crops by about 80% over the current level, which could benefit irrigators (Figure 5).

The mean number of days surface water reaches spring emergence is important for fisheries management. The only native trout in Teton Valley, Yellowstone cutthroat, migrate

upstream from the main Teton River in May and June to spawn (Koenig, 2006; Thurow et al., 1988). Emergent cutthroat trout fry migrate back to the main river late in the summer (Varley and Gresswell, 1988; Van Kirk et al., 2010). If there is no water remaining in the streams, these fish cannot complete their life cycle. The only tributary that naturally reaches spring emergence all year is Trail Creek (Figure 6). Under natural conditions, the other tributaries run dry by late September or early October (Figures 7-11). However, irrigation has reduced the number of days that surface flow provides a continuous fish migration route between the Teton River and tributary headwaters. I found that under the pipeline scenario, the mean number of days surface flow reaches spring emergence was greater than that under any of the other irrigation scenarios. Therefore, if keeping water in the stream channel for aquatic species is desirable, the pipeline scenario may offer restoration opportunities.

However, total groundwater recharge was lowest under the pipeline scenario, even less than under natural conditions. This is because under the pipeline scenario, there is no conveyance or application seepage, and there is less surface water left in the stream channel than under natural conditions to seep into the ground. Although placing all earthen canals in pipelines is more efficient, it can have negative consequences in Teton Valley. Some irrigators in the valley depend on emergent spring water down-gradient of the other canal systems, and many fish, wildlife and plant resources are maintained by springs that are recharged in part by irrigation seepage, as has been documented in other areas (Peck and Lovvorn, 2001; Peck et al., 2005). If canals are replaced with pipes, spring discharge would decrease, resulting in lower base flows in the Teton River.

Reductions in groundwater levels and resulting decreases in springflow have been observed in other areas where irrigation efficiency has been increased. According to Johnson et al. (1999), the reduction in groundwater levels in the Snake River Plain aquifer in southeast Idaho resulted partly from lining canals and converting to sprinkler irrigation.

Similarly, Boggs et al. (2010) used an analytical model to show that increasing irrigation efficiency in the Snake River Plain aquifer, in part, led to a steady decline in the Thousand Springs discharge further downstream. Miller et al. (2006) reported equivalent results using a simulation model on the Snake River Plain aquifer. Kendy and Bredehoeft (2006) indicated that improving irrigation efficiency reduced fall and winter base flows in the Gallatin River in western Montana. Venn et al. (2004) noted a 15 and 14 % decrease in flows in August and September, respectively, in the Salt River in Star Valley, Wyoming, after the conversion to sprinkler irrigation, coinciding with decreases in groundwater levels.

Regardless of whether the objective of a particular water management action is to increase, decrease or not change current hydrologic regimes and groundwater recharge in Teton Valley, my results show that recharge potential is greatest during wet years (Figure 25 top) but that the fraction of net flow through the valley that occurs in groundwater pathways is greatest during dry years (Figure 27 top). This implies that groundwater recharge during wet years helps maintain streamflow during dry years. The difference in total recharge across scenarios is greatest during wet years (Figure 25 bottom), implying that reductions in groundwater recharge due to increased irrigation efficiencies will be greatest in the wet years, when recharge potential is high. Conversely, the effect of changes in irrigation scenarios on overall hydrologic regimes are largest during the dry years (Figure 27 bottom), when streamflow at the bottom of the valley is most dependent on groundwater. Therefore, the potential effects of changes in irrigation practices on aquifer recharge will be greatest in wet years, and the effects on aquifer discharge back to the surface system will be greatest in dry years.

In conclusion, the introduction of irrigation systems in Teton Valley greatly increased groundwater recharge and the groundwater component of what naturally is a system dominated by surface runoff from snowmelt during the spring season. The hydrologic regime

can affect aquatic life, wildlife and riparian vegetation (Petts, 2009; Peck and Lovvorn, 2001; Peck et al., 2005; Poff et al., 1997; Richter et al., 1997). Replacing earthen canals with pipelines can move the hydrologic regime back toward the natural state in terms of the fraction of water flowing through the aquifer versus the surface water components, but at a cost of greatly decreased groundwater recharge. Regardless of whether irrigation water is used for agriculture or for uses associated with land development, changes in conveyance, not application, have the greatest potential effect on the hydrologic regime in Teton Valley. Whether these hydrologic changes are good or bad depends on the resources being considered.

This model will be used in further studies. The recharge and surface flow components and surface flow are inputs to a larger flow model. The surface water/groundwater interactions are important for the larger Henry's Fork watershed, of which Teton Valley is a subwatershed. This work, combined with another concurrent study, will be used to develop the lower Henry's Fork watershed model.

BIBLIOGRAPHY

Allen, R. and C. Robison. 2009. Evapotranspiration and consumptive irrigation water requirements for Idaho: Supplement updating the time series through December 2008. Tech. rep. Research Technical Completion Report, Kimberly Research and Extension Center, University of Idaho, Moscow, ID. Data available at http://www.kimberly.uidaho.edu/ETIdaho/.

Boggs, K., R. Van Kirk, G. Johnson, J. Fairley, and S. Porter. 2010. Analtyical solutions to the linearized Boussinesq equation for assessing the effects of recharge on aquifer discharge. *Journal of the American Water Resources Association*, **46**(6):1116–1132.

Burnham, K. P. and D. R. Anderson. 2002. *Model Selection and Multimodel Inference*. 2nd ed., Springer, New York.

Burt, C., A. Clemmens, T. Strelkoff, K. Solomon, R. Bliesner, L. Hardy, T. Howell, Members of ASCE, and D. Eisenhauer. 1997. Irrigation performance measures: Efficiency and uniformity. *Journal of Irrigation and Drainage Engineering*, **123**(6):423–442.

Contor, B. 2004. Delineation of sprinkler and gravity application systems. Idaho Falls, ID 2004-005. Idaho Water Resources Research Institute 200804.

Contor, B. 2008. Representation of recharge from canal leakage for calibration of Eastern Snake Plain aquifer model version 2. Submitted to University of Idaho. Idaho Water Resources Research Institute 200804.

Fetter, C. 1994. *Applied Hydrogeology*. 3rd Ed. Macmillan College Publishing Company, Inc. New York.

Fiege, M. 1999. *Irrigated Eden: The making of an agricultural landscape in the American West*. University of Washington Press, Seattle.

Friends of the Teton River. 2009. Upper Teton River model wathershed project proposal. Submitted to The Boneville Environmental Foundation. Portland, OR.

Helmus, A., A. Fernald, D. VanLeeuwen, L. Abbott, A. Ulery, and T. Baker. 2009. Surface water seepage effects on shallow ground-water quality along the Rio Grande in northern New Mexico. *Journal of the American Water Resources Association*, **45**(2):407–418.

Hermance, J. 1999. *A Mathematical Primer on Groundwater Flow: An Introduction to the Mathematical and Physical Concepts of Saturated Flow in the Subsurface*. Prentice Hall. New Jersey.

Johnson, G., W. Sullivan, D. Cosgrove, and R. Schmidt. 1999. Recharge of the Snake River Plain aquifer: Transitioning from incidental to managed. *Journal of the American Water Resources Association*, **35**(1):123–131.

Kendy, E. and J. Bredehoeft. 2006. Transient effects of groundwater pumping and surface-water-irrigation returns on streamflow. *Water Resources Research*, **42**. W08415, DOI: 10.1029/2005WR004792.

Kilburn, C. 1964. Ground water in the upper part ot the Teton Valley, Teton counties, Idaho and Wyoming. *US Geological Survey Water Supply Paper: 1789*. US Government Printing Office, Washington, D.C.

Knight, J., M. Gilfedder, and G. Walker. 2004. Impacts of irrigation and dryland development on groundwater discharge to rivers-a unit response approach to cumulative impacts analysis. *Journal of Hydrology*, **303**(2005):79–91.

Koenig, M. K. 2006. *Habitat and biotic factors influencing the distribution and recruitment of juvenile cutthroat trout in the Teton River, Idaho.* Master's thesis, Utah State University, Logan, UT.

Liegel, L. H. 2011. *Landscapes in transition: exploring the intersections between land use planning and water management in the Henry's Fork Watershed, Idaho.* Master's thesis, Environment and Community Program Humboldt State University, Arcata, CA.

Liu, C., H. Huang, S. Chen, and Y. Kuo. 2004. Subsurface return flow and ground water recharge of terrace fields in northern Taiwan. *Journal of the American Water Resources Association*, **40**(3):603–614.

Love, J., J. Reed, J. Pierce, and K. Pierce. 2003. *Creation of the Teton Landscape: A Geological Chronicle of Jackson Hole and the Teton Range*. Grand Teton Natural History Association, Moose, WY.

Miller, S., G. Johnson, D. Cosgrove, and R. Larson. 2006. Regional scale modeling of surface and ground water interaction in the Snake River basin. *Journal of the American Water Resources Association*, **39**(3):517–528.

Nicklin Earth and Water, Inc. 2003. Ground-water model for the upper Teton watershed. Submitted to Cascade Earth Sciences, Inc., Pocatello, ID. Nicklin Earth and Water, Inc., Bozeman, MT.

Peck, D. and J. Lovvorn. 2001. The importance of flood irrigation in water supply to wetlands in the Laramie Basin, Wyoming, USA. *Wetlands*, **21**:370–378.

Peck, D., D. Mcleod, J. Hewlett, and J. Lovvorn. 2005. Irrigation-dependent wetlands versus instream flow enhancement: Economics of water transfers from agriculture to wildlife uses. *Environmental Management*, **34**:842–855.

Petts, G. 2009. Instream flow science for sustainable river management. *Journal of the American Water Resources Association*, **45**:1071–1086.

Poff, N., J. Allen, M. Bain, J. Karr, K. Prestegaard, B. Richter, R. Sparks, and J. Stromberg. 1997. The natural flow regime a paradigm for conservation and restoration. *BioScience*, **47**:769–784.

Richter, B. D., J. V. Baumgartner, R. Wigington, and D. P. Braun. 1997. How much water does a river need? *Freshwater Biology*, **37**:231–249.

Richter, B. D., R. Mathews, D. L. Harrison, , and R. Wigington. 2003. Ecologically sustainable water management: managing river flows for ecological integrity. *Ecological Applications*, **13**:206–224.

Thurow, R. F., C. E. Corsi, and V. K. Moore. 1988. Status, ecology and management of Yellowstone cutthroat trout in the upper Snake River drainage, Idaho. *American Fisheries Society Symposium*, **4**:25–36.

Van Kirk, R. 2008. Conservation of surface and ground water in a western watershed experiencing rapid loss of irrigated agricultural land to development. Submitted to the Integrated Research,, Education, and Extension Competitive Grants Program, National Integrated Water Quality Program, USDA.

Van Kirk, R. and L. Benjamin. 2000. Physical and human geography of the Henry's Fork watershed. *Intermountain Journal of Sciences*, **6**(3):106–118.

Van Kirk, R. and A. Jenkins. 2005. Hydrologic alteration in the upper Teton watershed and its implications for cutthroat trout restoration. Report for Friends of the Teton River, Driggs, ID. 72 pp.

Van Kirk, R. W., L. Battle, and W. C. Schrader. 2010. Modelling competition and hybridization between native cutthroat trout and nonnative rainbow and hybrid trout. *Journal of Biological Dynamics*, **4**:158–175.

Varley, J. D. and R. E. Gresswell. 1988. Ecology, status and management of the yellowstone cutthroat trout. *American Fisheries Society Symposium*, **4**:13–24.

Venn, B., D. Johnson, and L. Pochop. 2004. Hydrologic impacts due to changes in conveyance and conversion from flood to sprinkler irrigation practices. *Journal of Irrigation and Drainage Engineering*, **130**(3):192–200.

Wytzes, J. 1980. Development of a groundwater model for the Henry's Fork and Rigby fan areas, upper Snake River basin, Idaho. *Ph.D. Dissertation, Department of Civil Engineering, University of Idaho*. 196 pp.

Zalidis, G., X. Dimitriadis, A. Antonopoulos, and A. Gerakis. 1997. Estimation of a network irrigation efficiency to cope with reduced water supply. *Irrigation and Drainage Systems*, **11**:337–345.

FIGURES

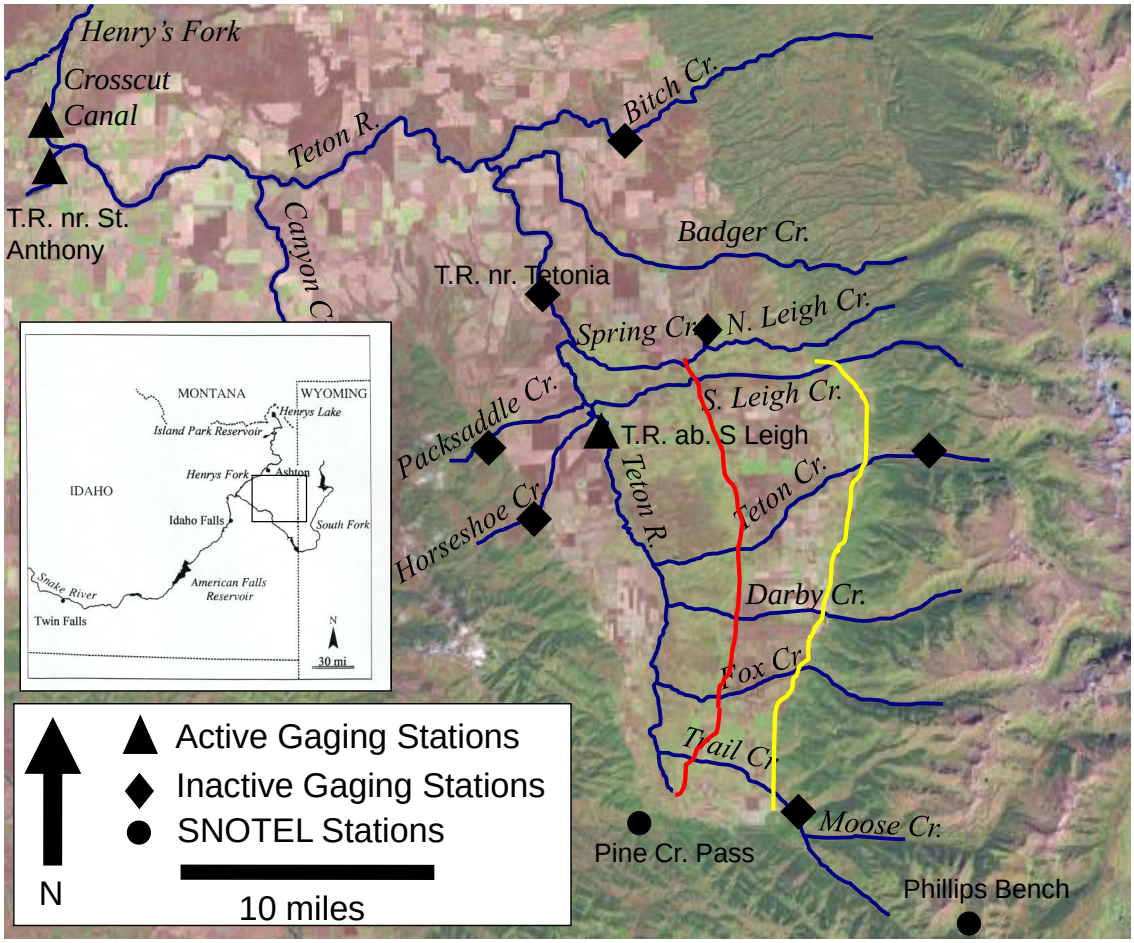

Figure 1: Map of Teton Valley. The orange line is the location of the top of the alluvial fans. The red line indicates the location of spring emergence.

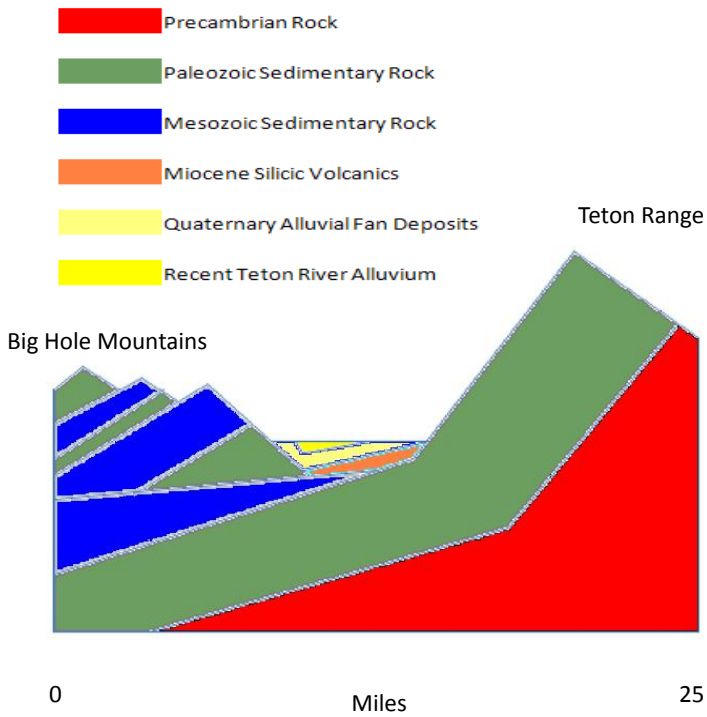

Figure 2: Idealized geologic cross section of Teton Valley. Vertical scale is exaggerated.

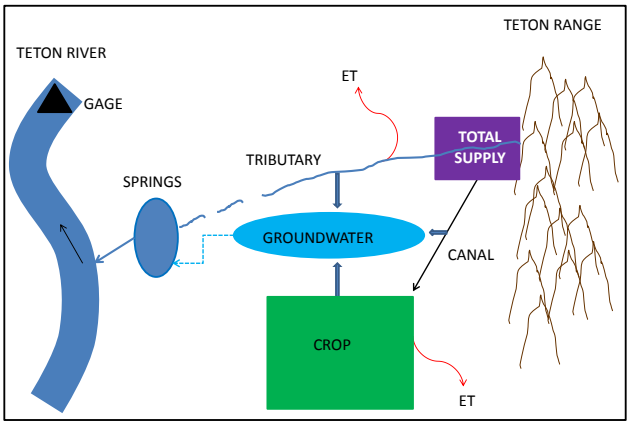

Figure 3: A schematic of water flow through the model domain.

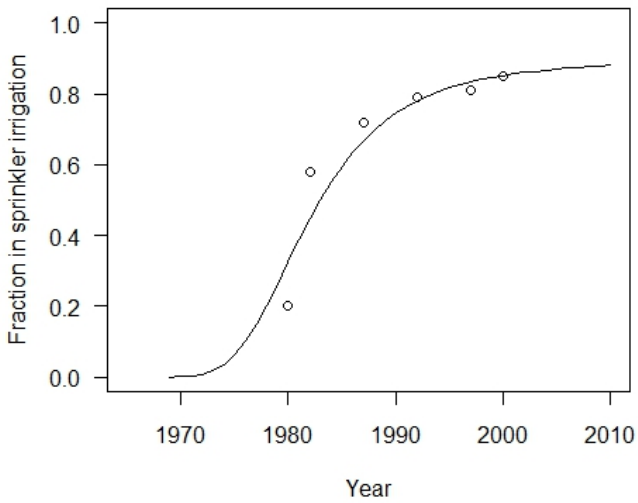

Figure 4: Observed (Contor 2004) and modeled (Equation 26) fraction of land in sprinkler irrigation.

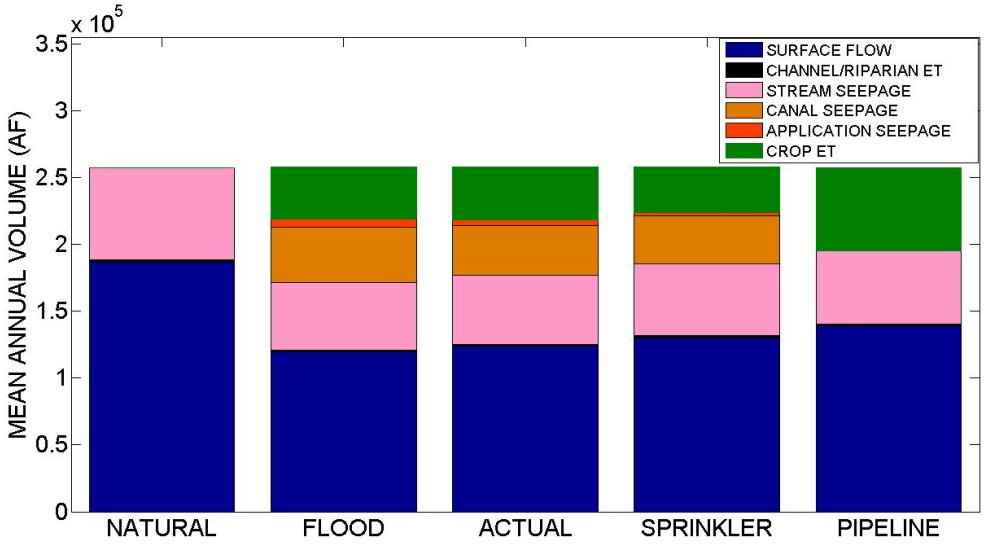

Figure 5: Total water budget for inflow from the six major Teton Valley streams.

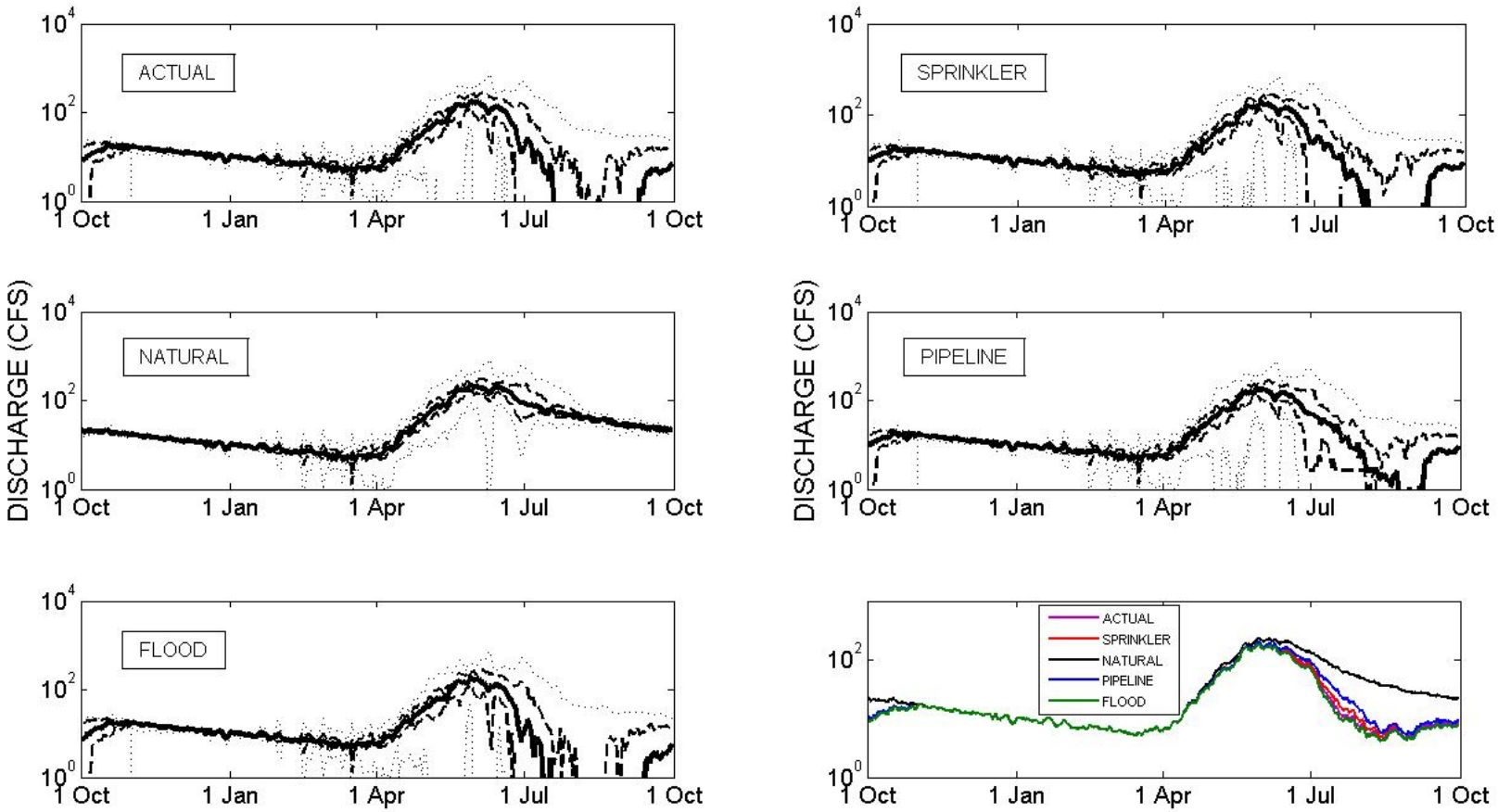

Figure 6: Trail Creek hydrographs: The first five panels depict the five number summary of daily flow over the 30 water years for the corresponding scenarios; the lower right panel compares scenario means (note this panel has a different vertical scale than the other five panels).

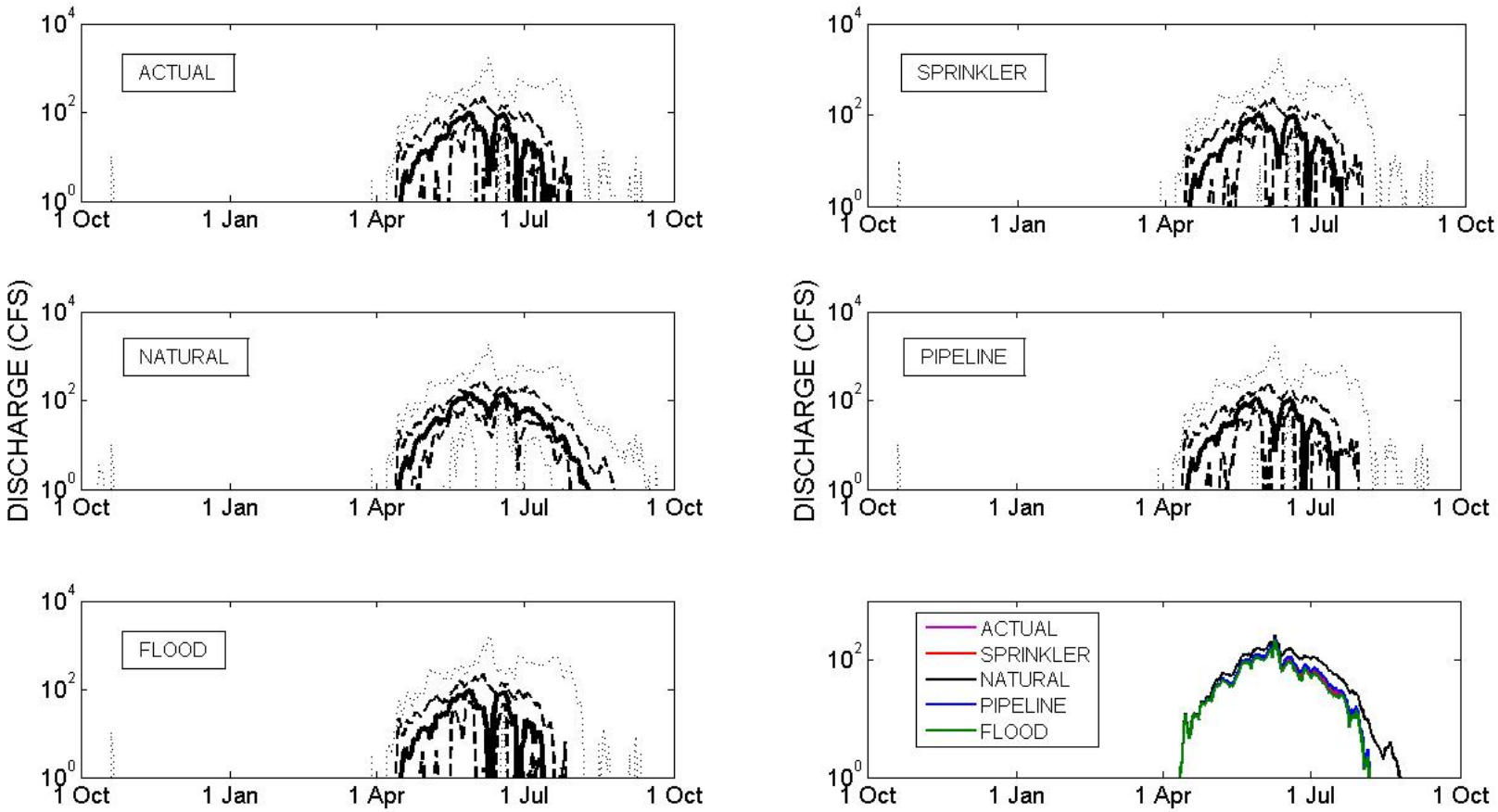

Figure 7: Fox Creek hydrographs: The first five panels depict the five number summary of daily flow over the 30 water years for the corresponding scenarios; the lower right panel compares scenario means (note this panel has a different vertical scale than the other five panels).

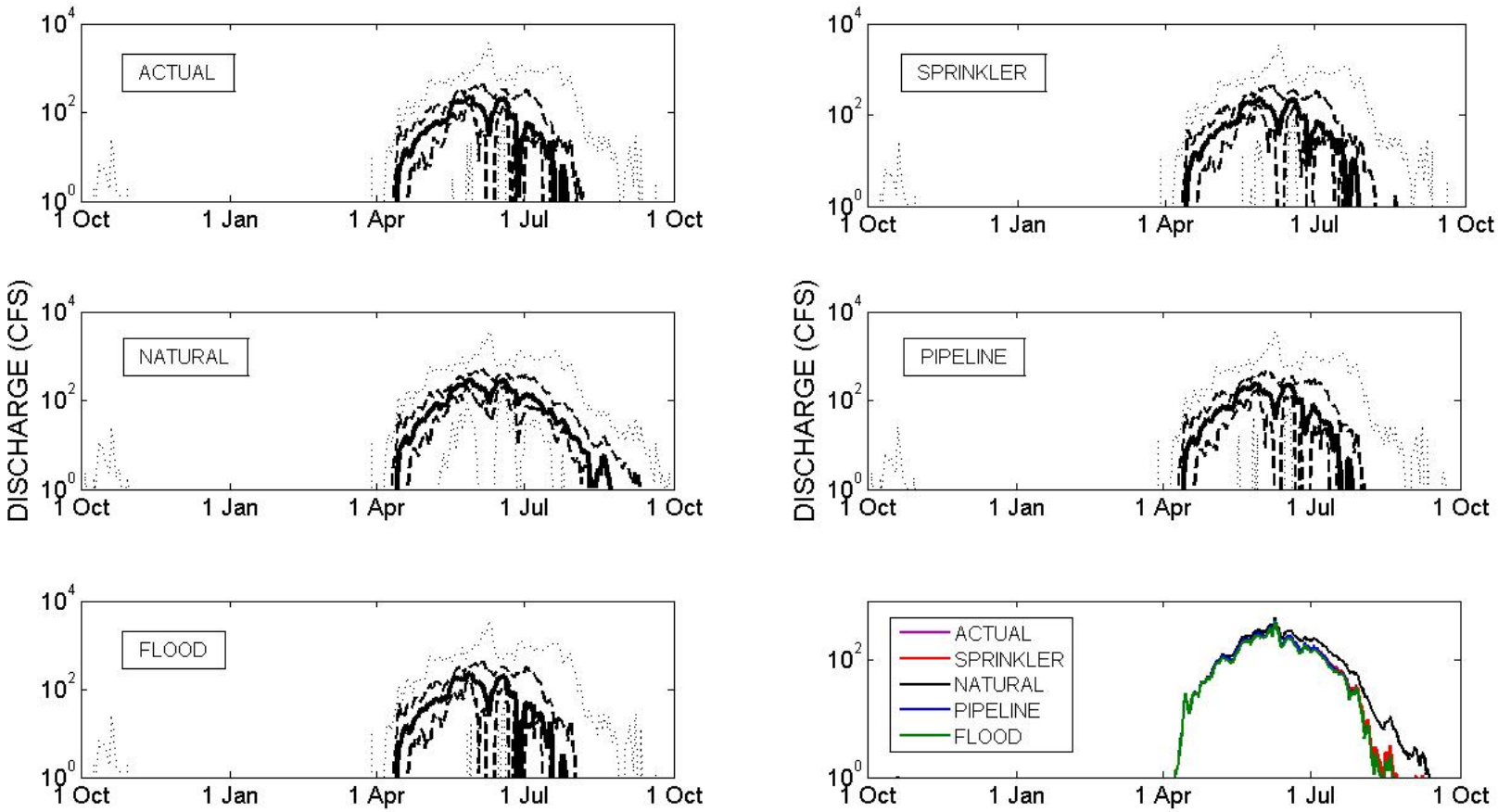

Figure 8: Darby Creek hydrographs: The first five panels depict the five number summary of daily flow over the 30 water years for the corresponding scenarios; the lower right panel compares scenario means (note this panel has a different vertical scale than the other five panels).

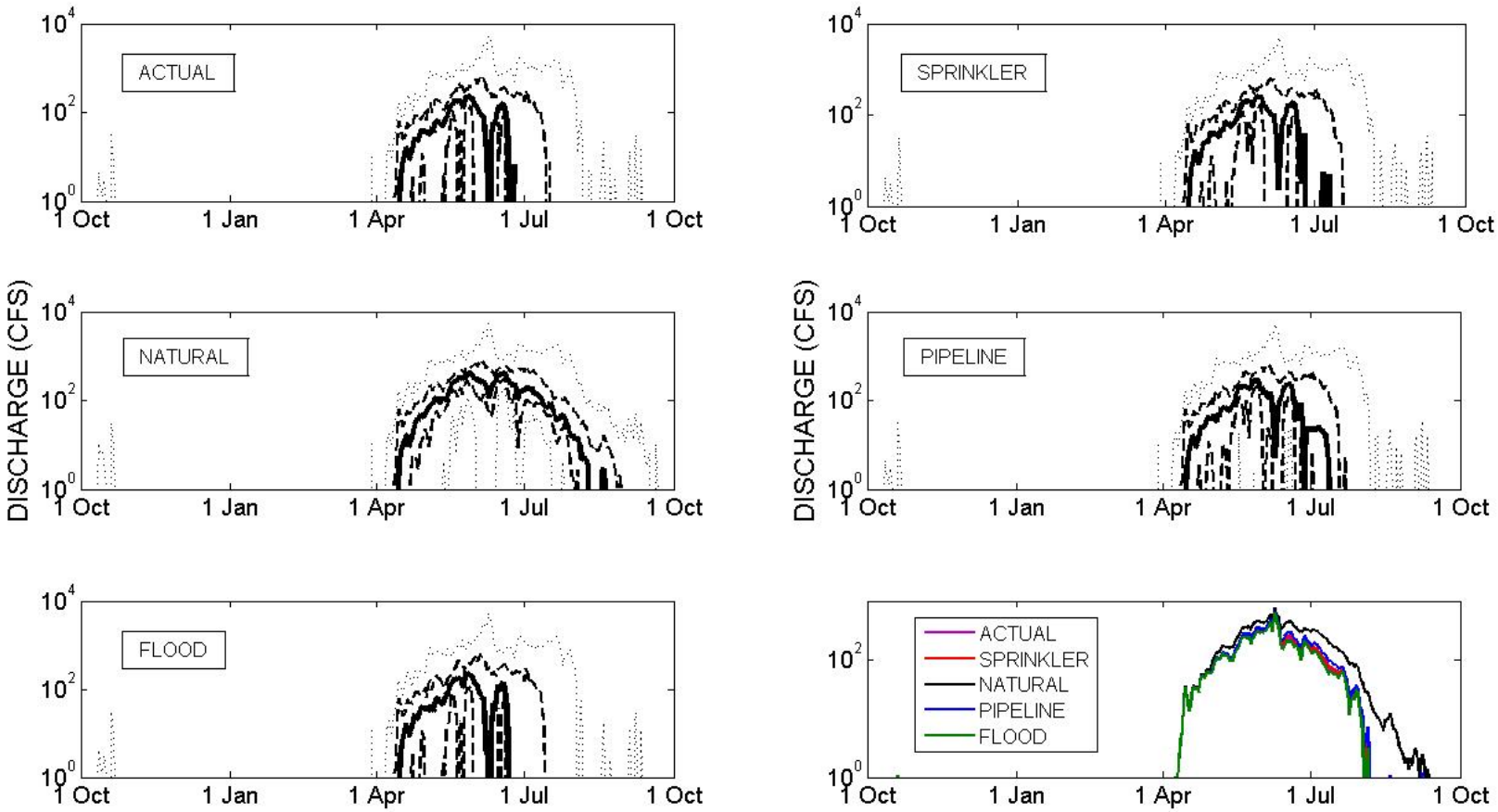

Figure 9: Teton Creek hydrographs: The first five panels depict the five number summary of daily flow over the 30 water years for the corresponding scenarios; the lower right panel compares scenario means (note this panel has a different vertical scale than the other five panels).

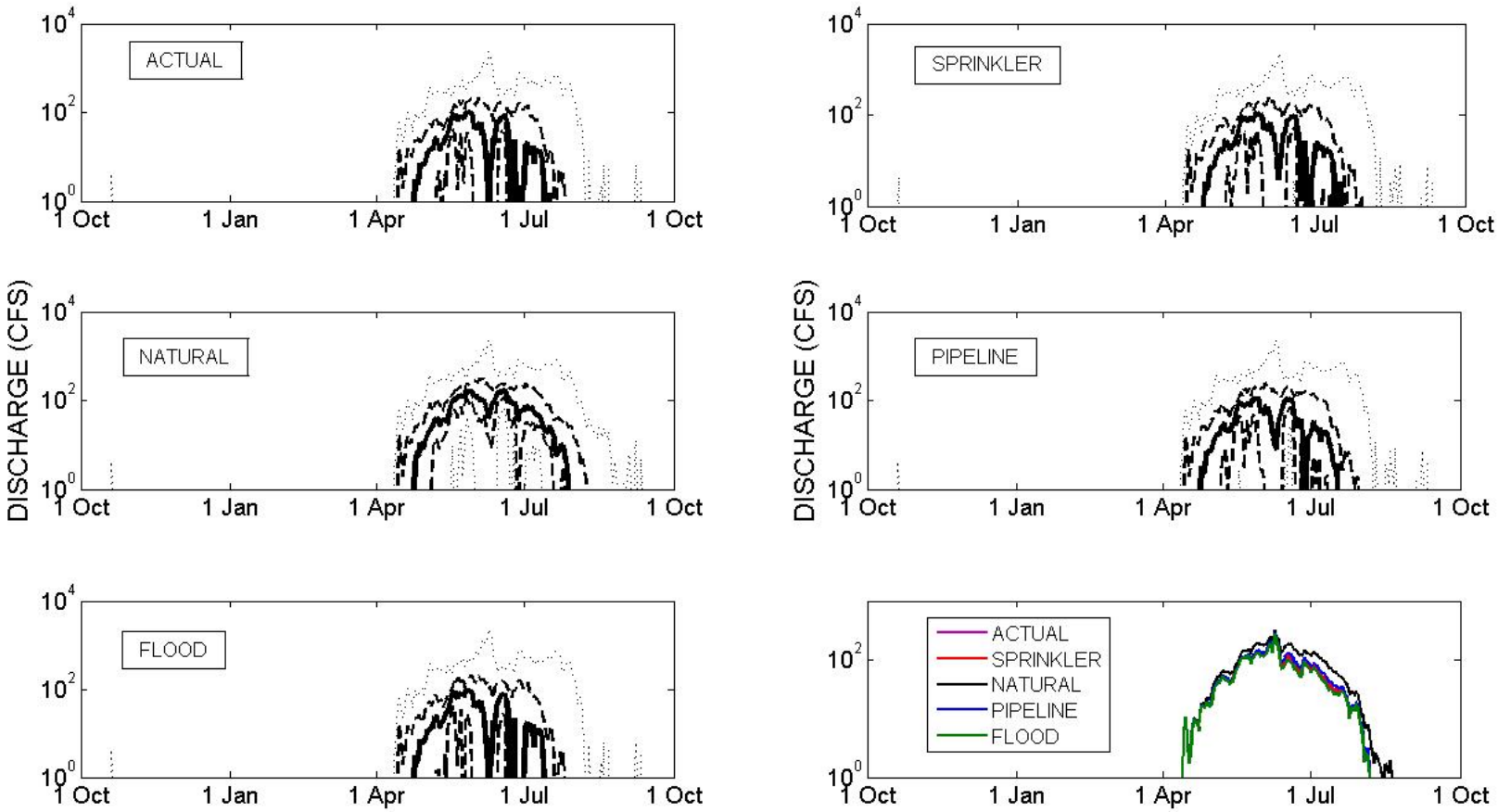

Figure 10: South Leigh Creek hydrographs: The first five panels depict the five number summary of daily flow over the 30 water years for the corresponding scenarios; the lower right panel compares scenario means (note this panel has a different vertical scale than the other five panels).

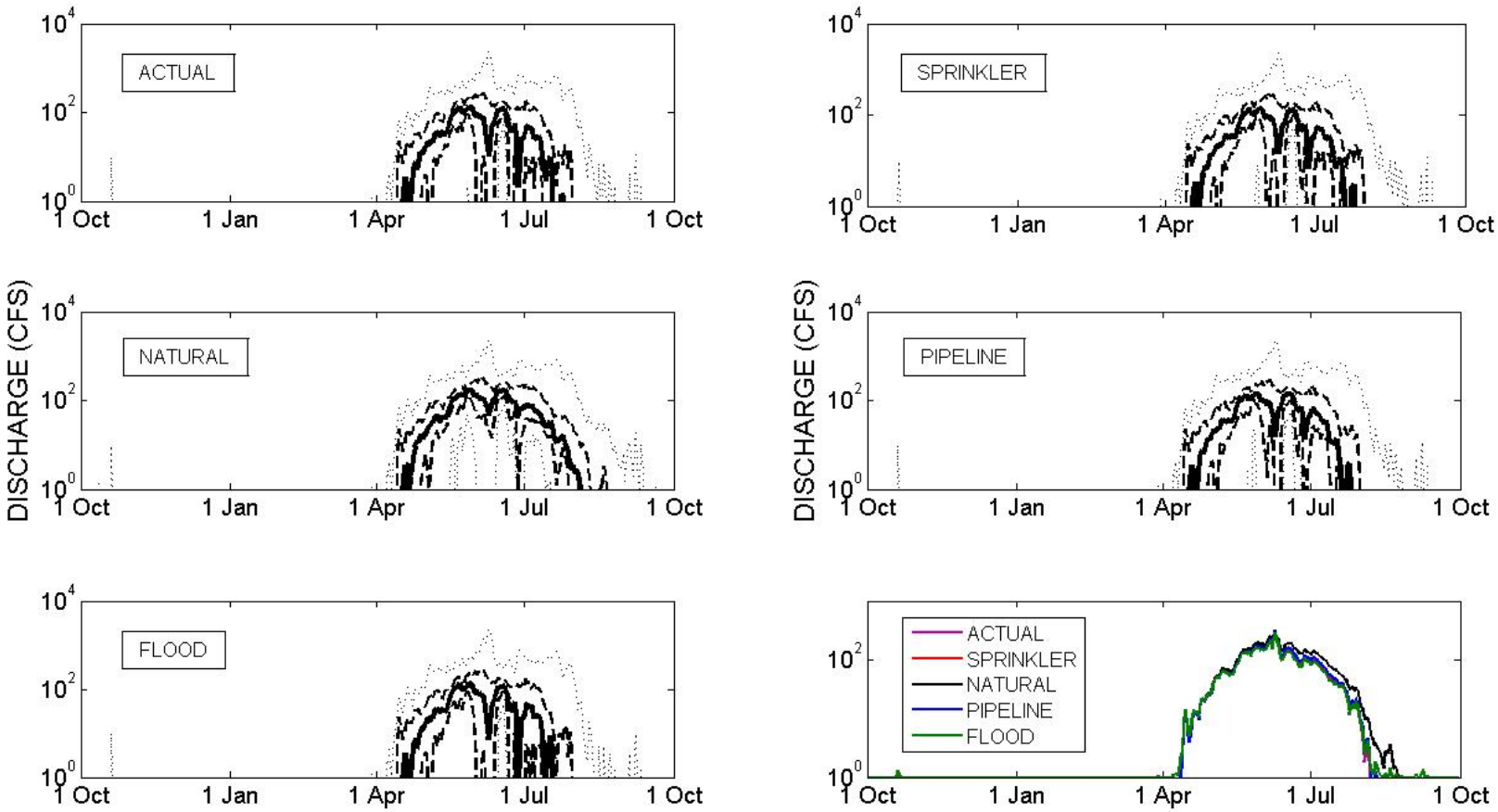

Figure 11: North Leigh Creek hydrographs: The first five panels depict the five number summary of daily flow over the 30 water years for the corresponding scenarios; the lower right panel compares scenario means (note this panel has a different vertical scale than the other five panels).

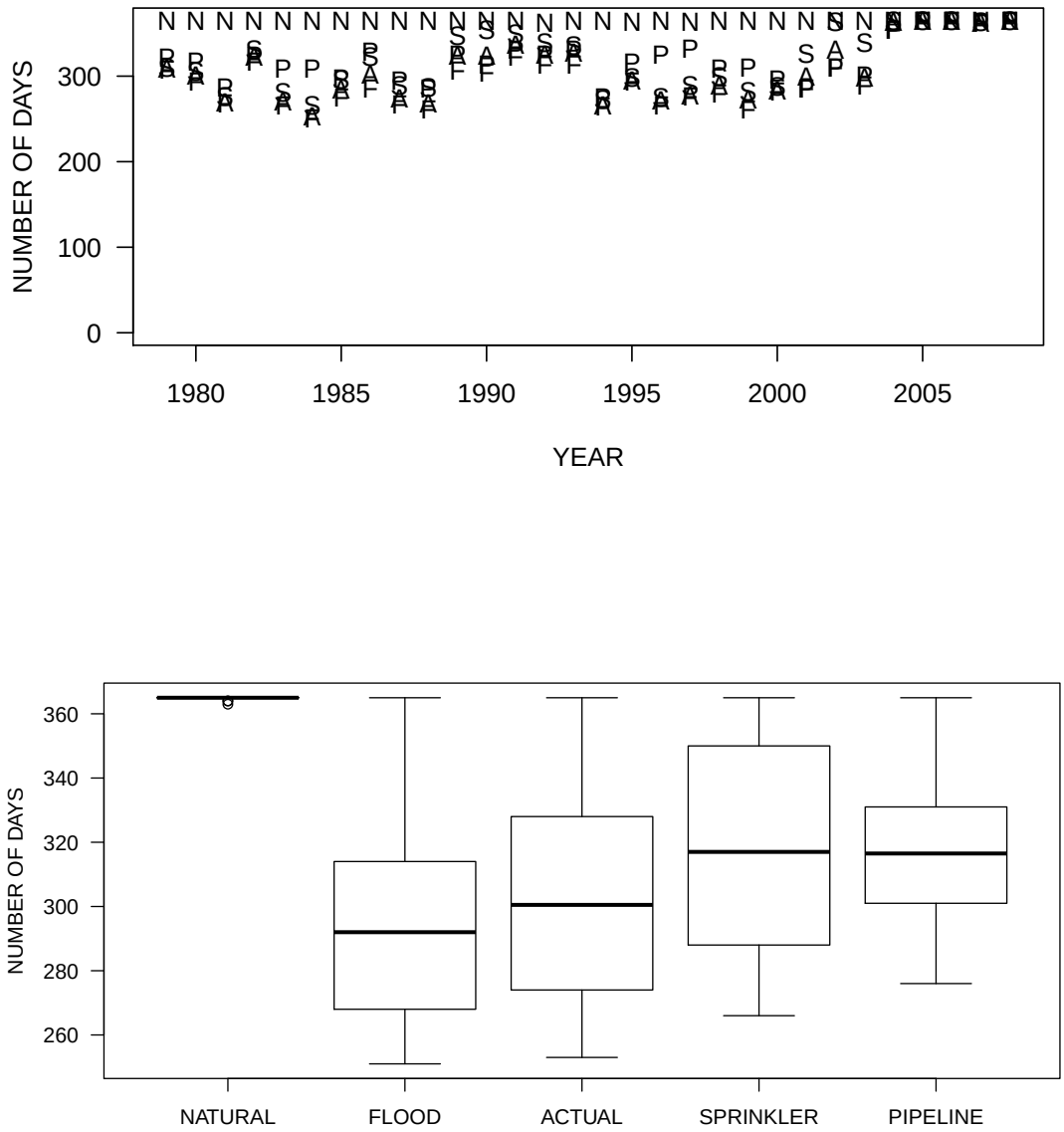

Figure 12: Number of days Trail Creek surface flow reaches point of spring emergence under each water year (top), and summarized over water years (bottom), by scenario. N = Natural, F = Flood, A = Actual, S = Sprinkler, P = Pipeline.

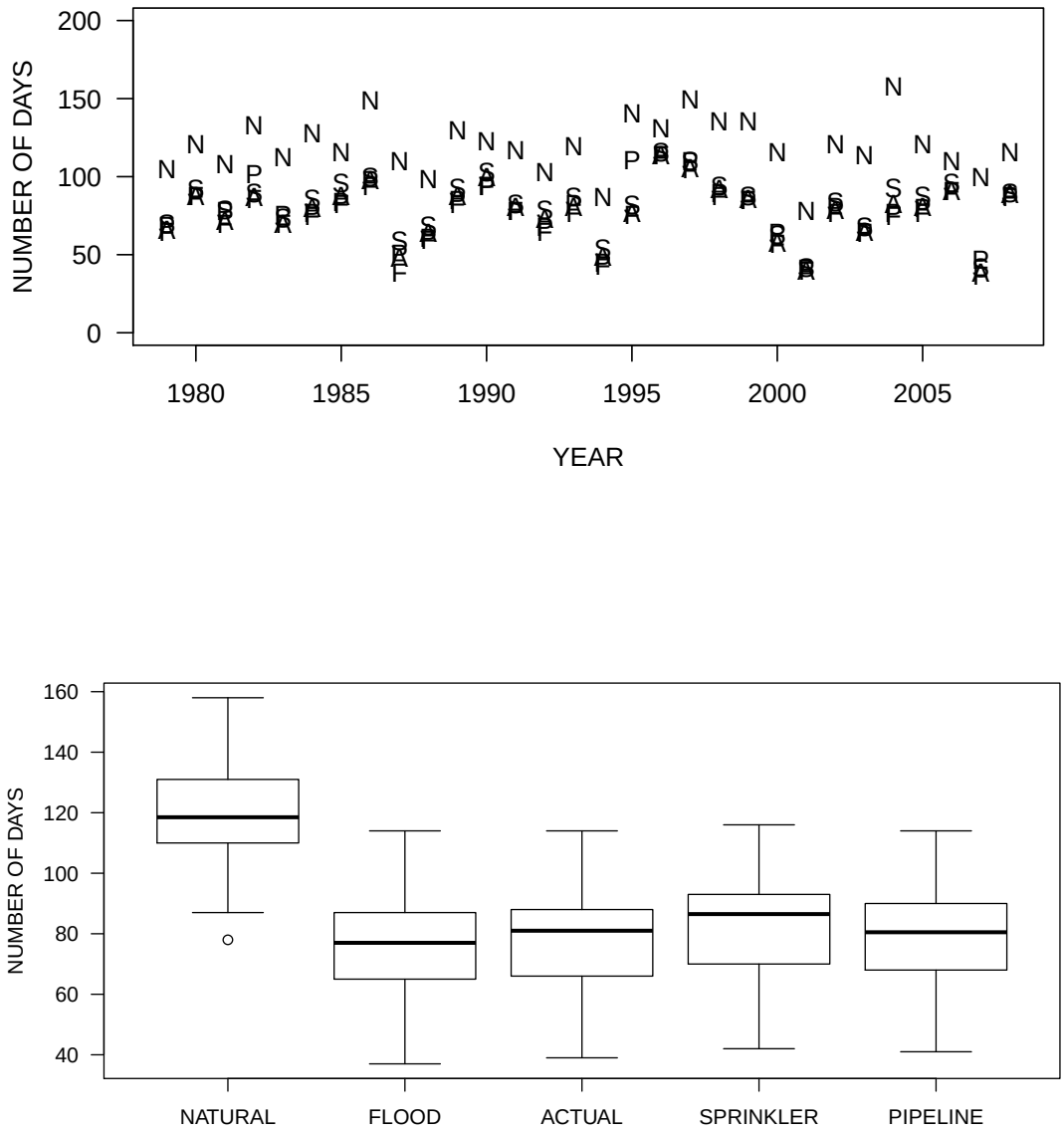

Figure 13: Number of days Fox Creek surface flow reaches point of spring emergence under each water year (top), and summarized over water years (bottom), by scenario. N = Natural, F = Flood, A = Actual, S = Sprinkler, P = Pipeline.

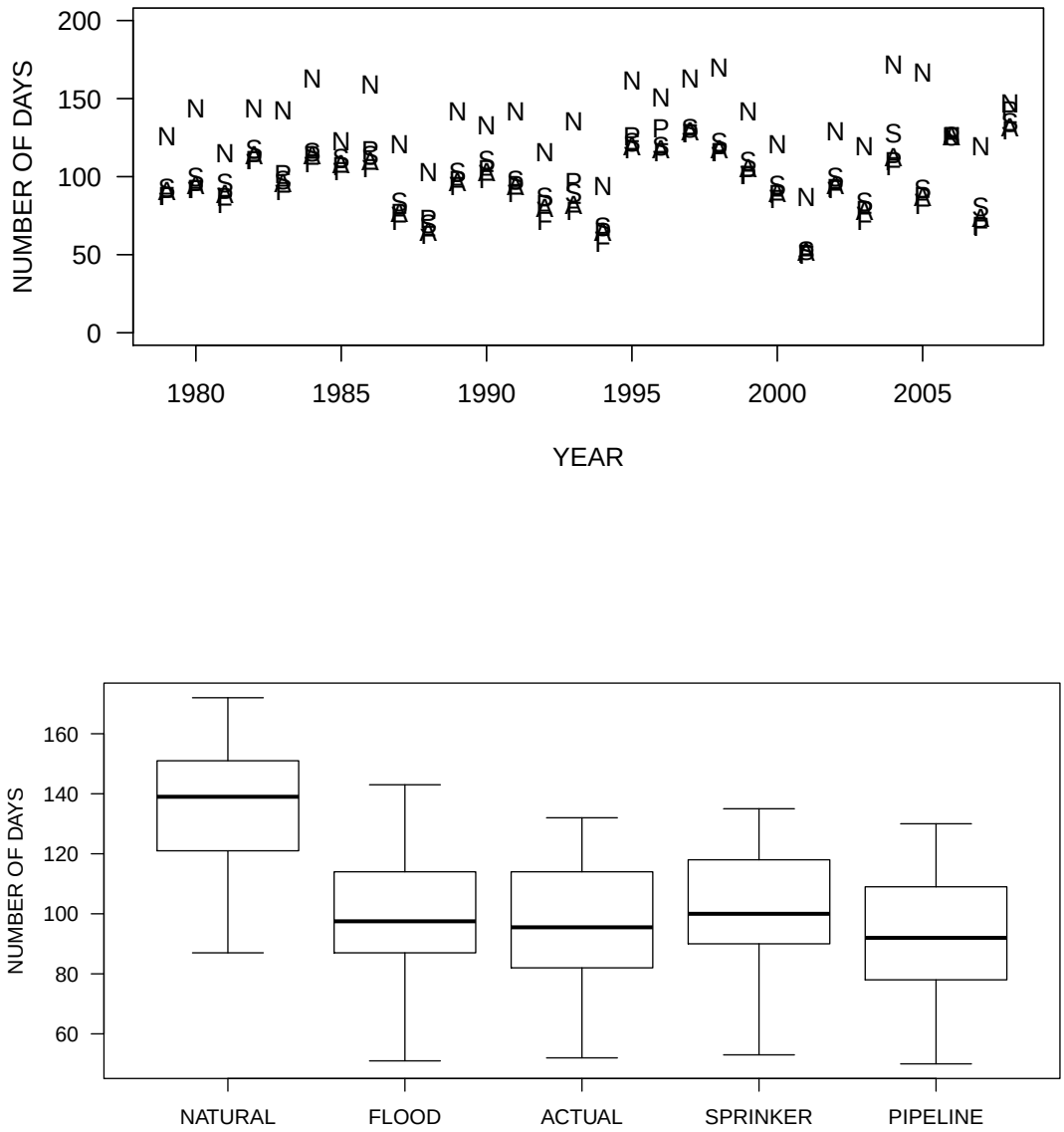

Figure 14: Number of days Darby Creek surface flow reaches point of spring emergence under each water year (top), and summarized over water years (bottom), by scenario. N = Natural, F = Flood, A = Actual, S = Sprinkler, P = Pipeline.

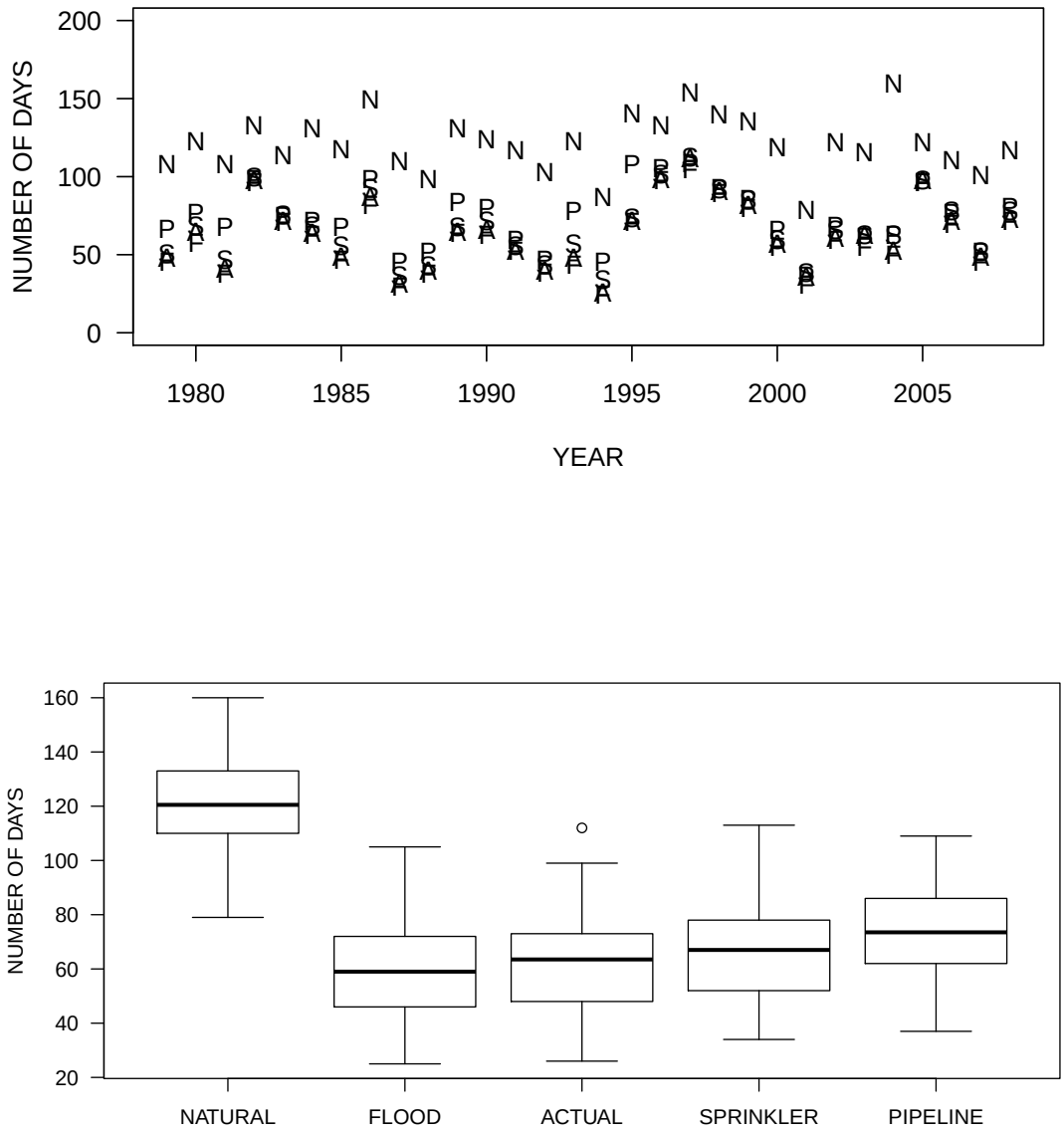

Figure 15: Number of days Teton Creek surface flow reaches point of spring emergence under each water year (top), and summarized over water years (bottom), by scenario. N = Natural, F = Flood, A = Actual, S = Sprinkler, P = Pipeline.

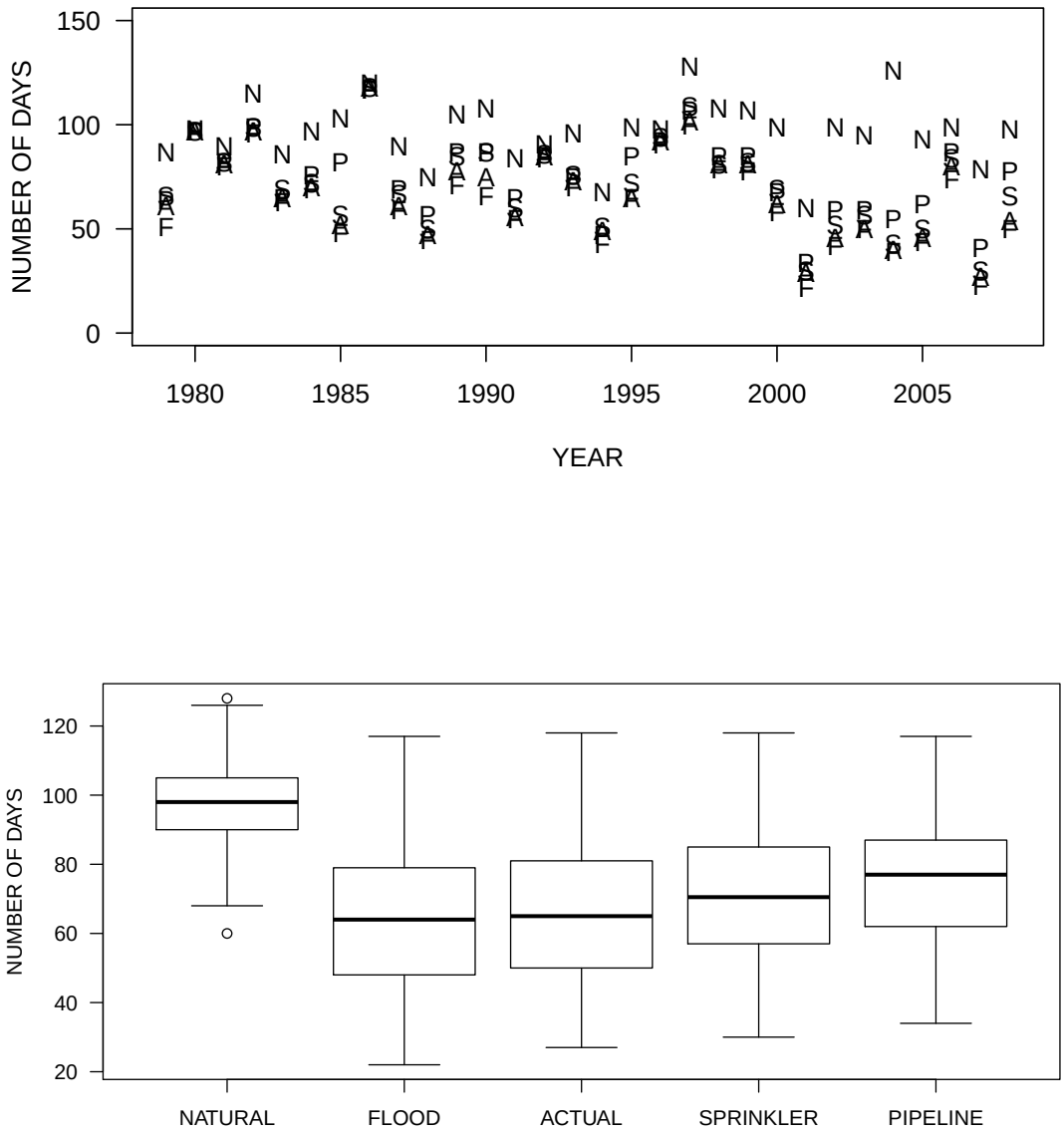

Figure 16: Number of days South Leigh Creek surface flow reaches point of spring emergence under each water year (top), and summarized over water years (bottom), by scenario. N = Natural, F = Flood, A = Actual, S = Sprinkler, P = Pipeline.

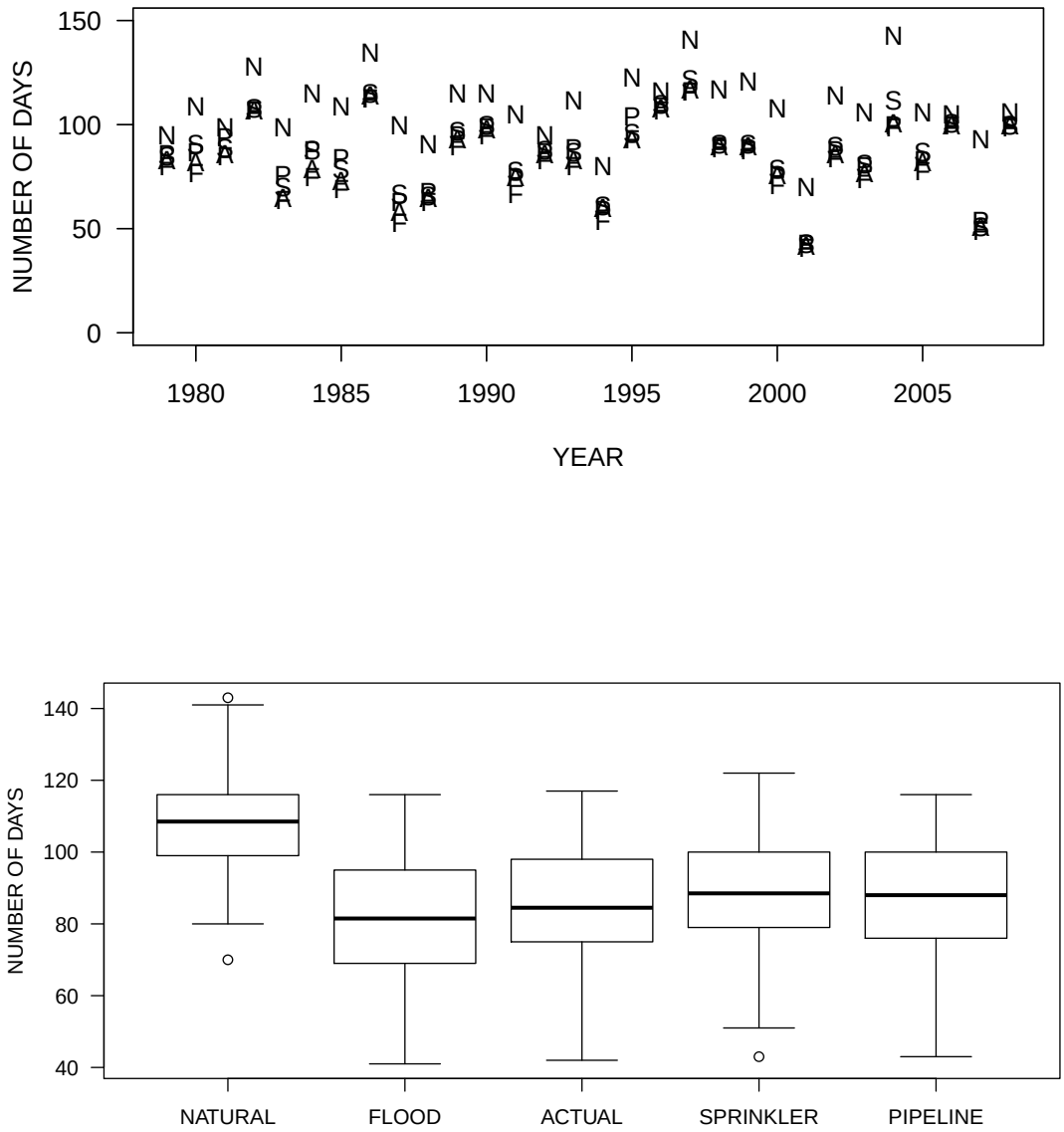

Figure 17: Number of days North Leigh Creek surface flow reaches point of spring emergence under each water year (top), and summarized over water years (bottom), by scenario. N = Natural, F = Flood, A = Actual, S = Sprinkler, P = Pipeline.

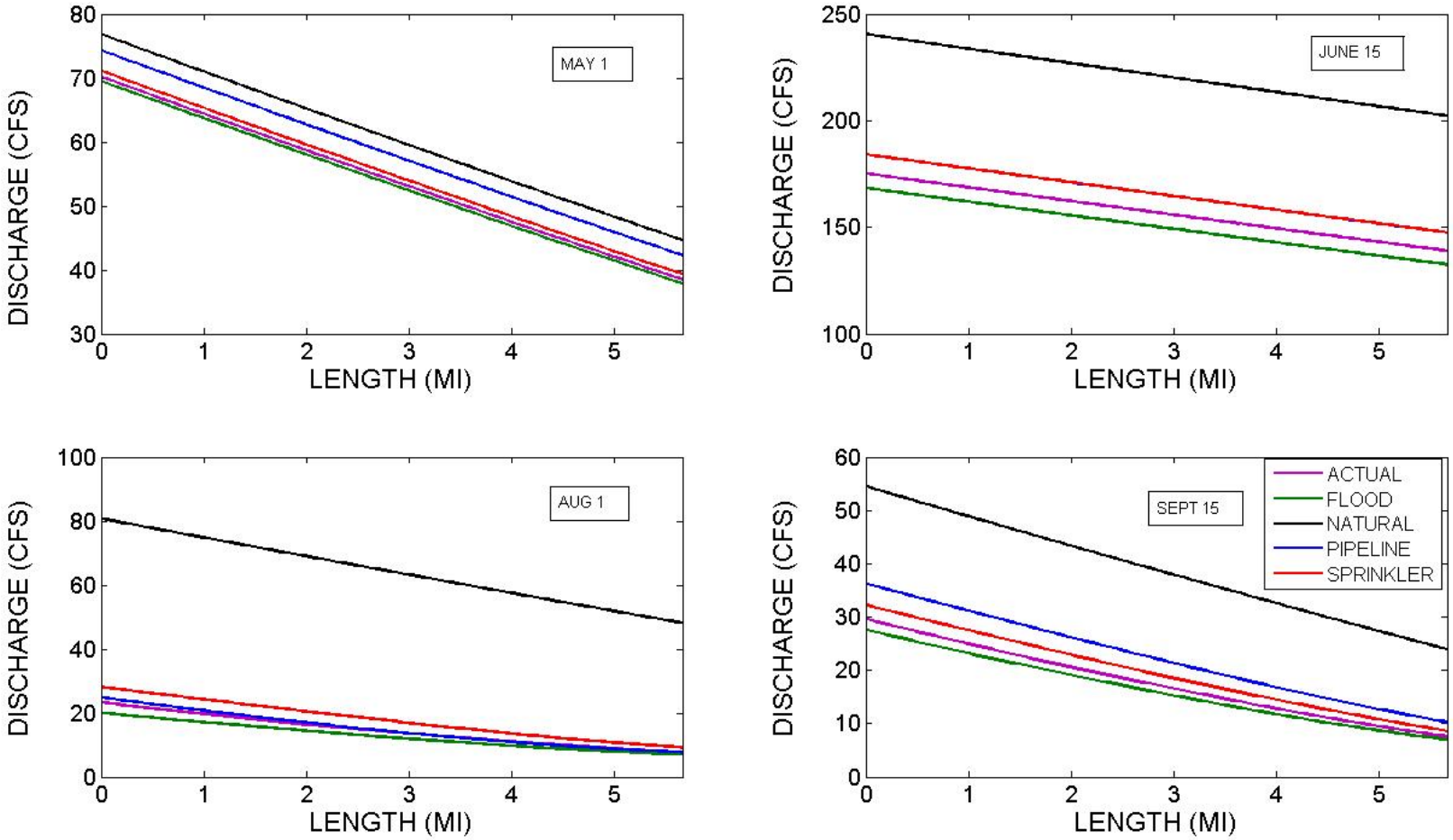

Figure 18: Mean discharge in Trail Creek versus distance across alluvial fan reach on the respective days.

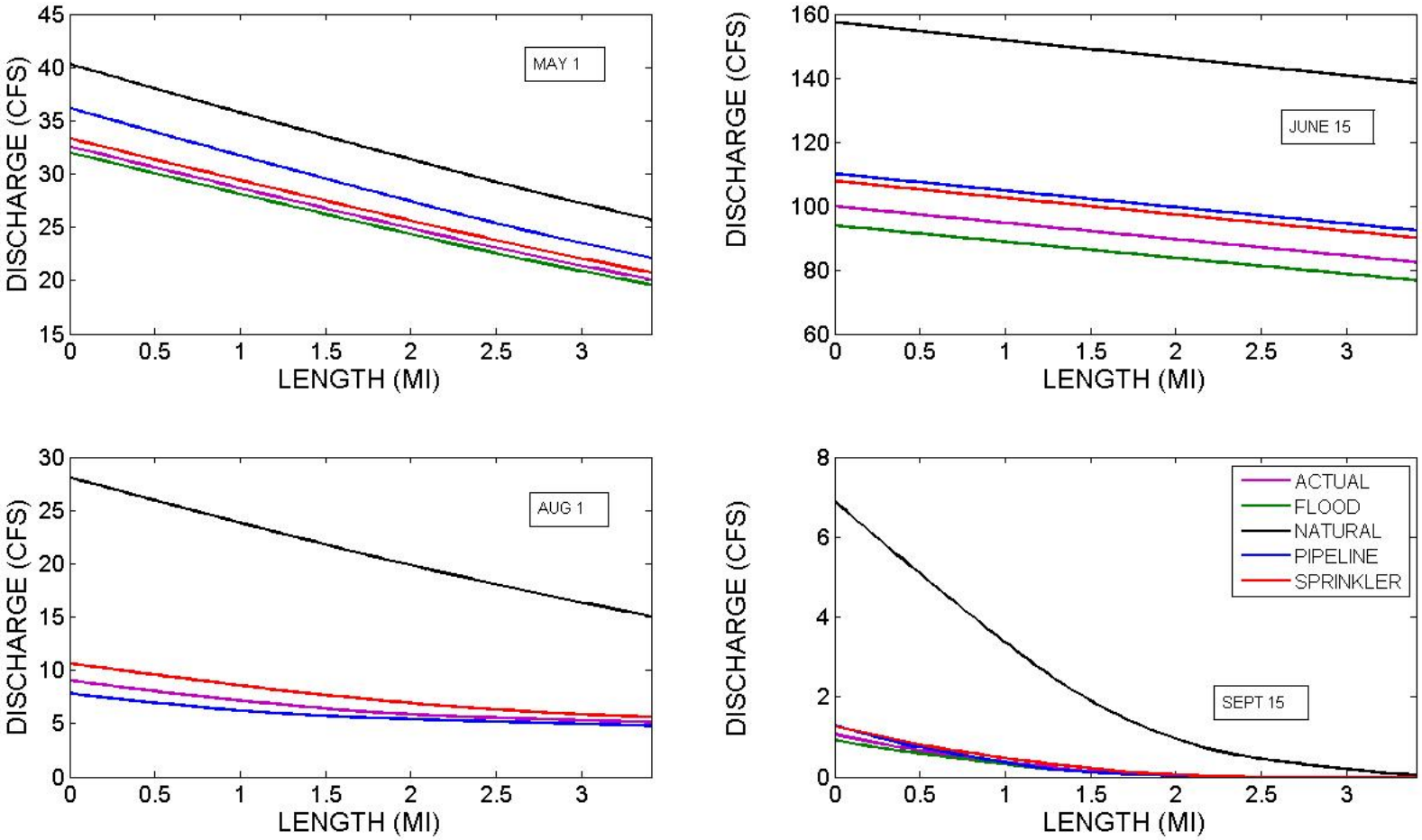

Figure 19: Mean discharge in Fox Creek versus distance across alluvial fan reach on the respective days.

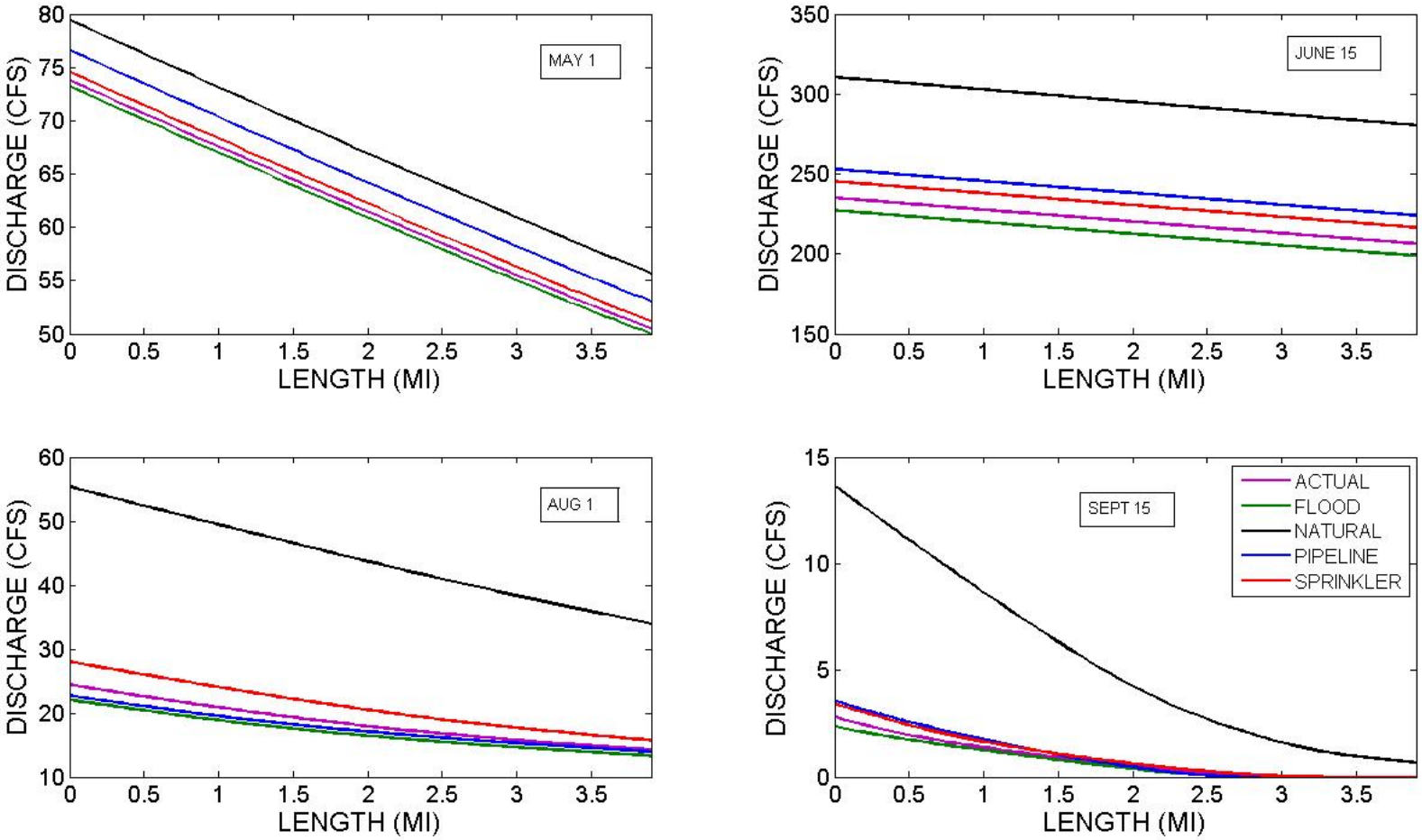

Figure 20: Mean discharge in Darby Creek versus distance across alluvial fan reach on the respective days.

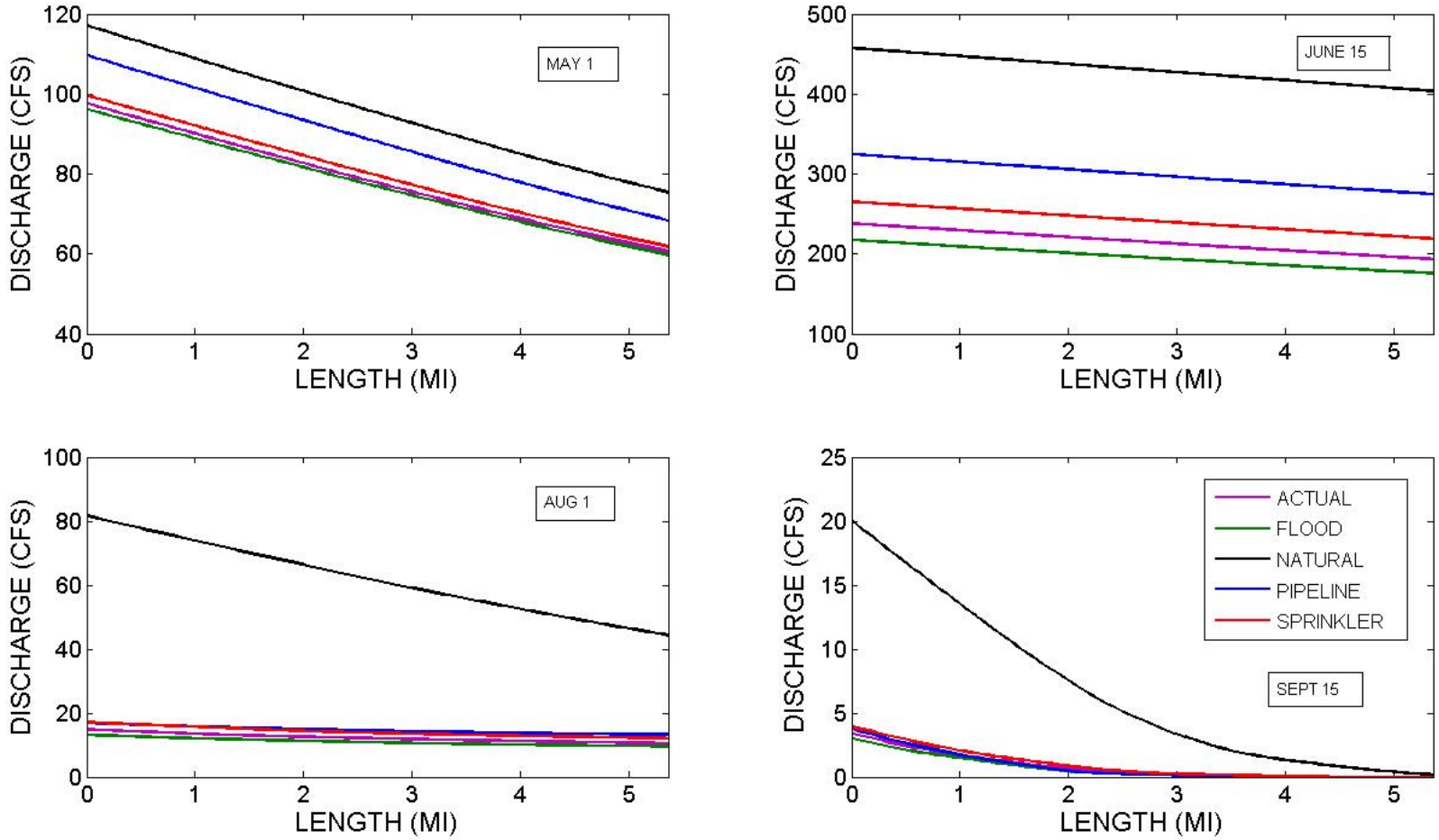

Figure 21: Mean discharge in Teton Creek versus distance across alluvial fan reach on the respective days.

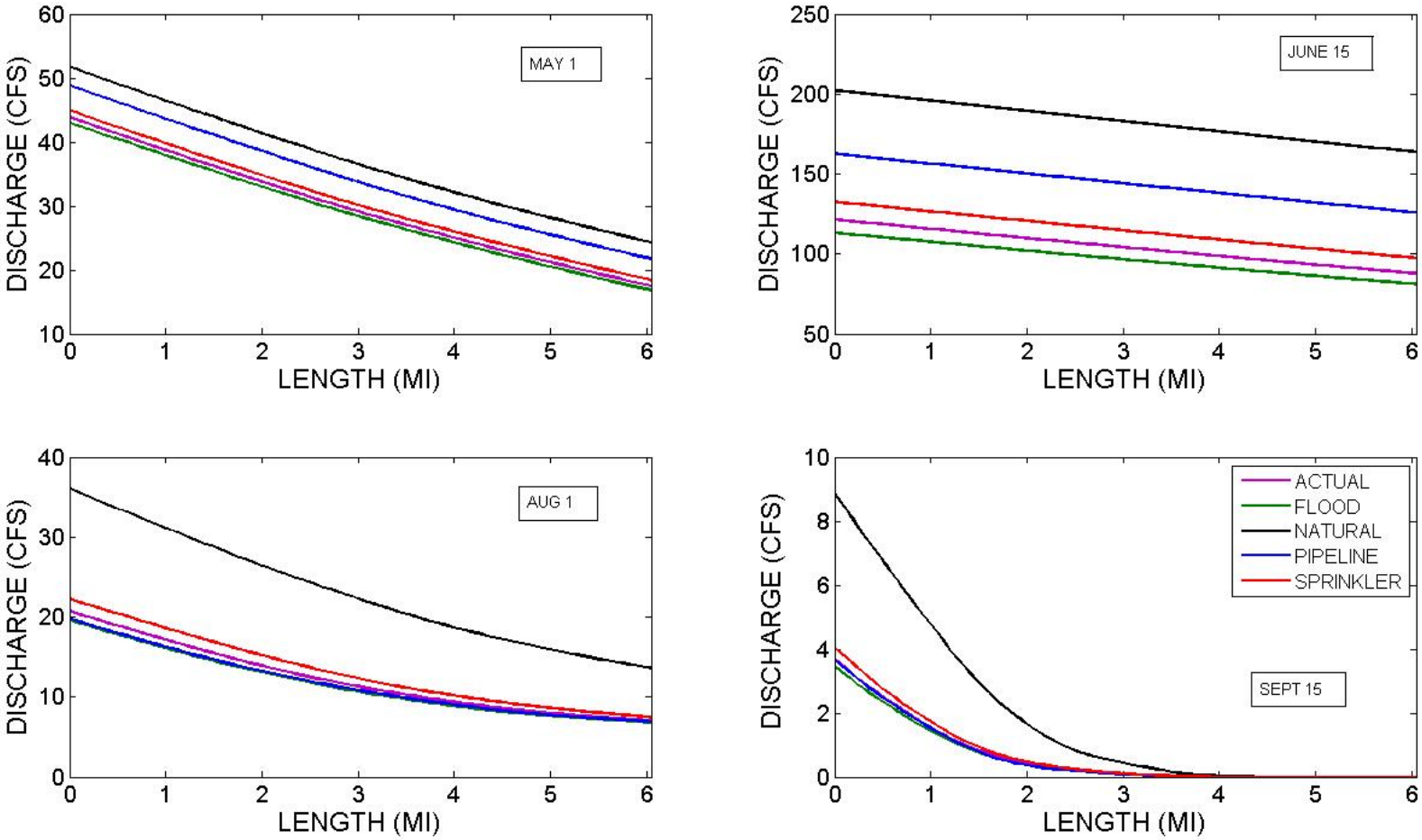

Figure 22: Mean discharge in South Leigh Creek versus distance across alluvial fan reach on the respective days.

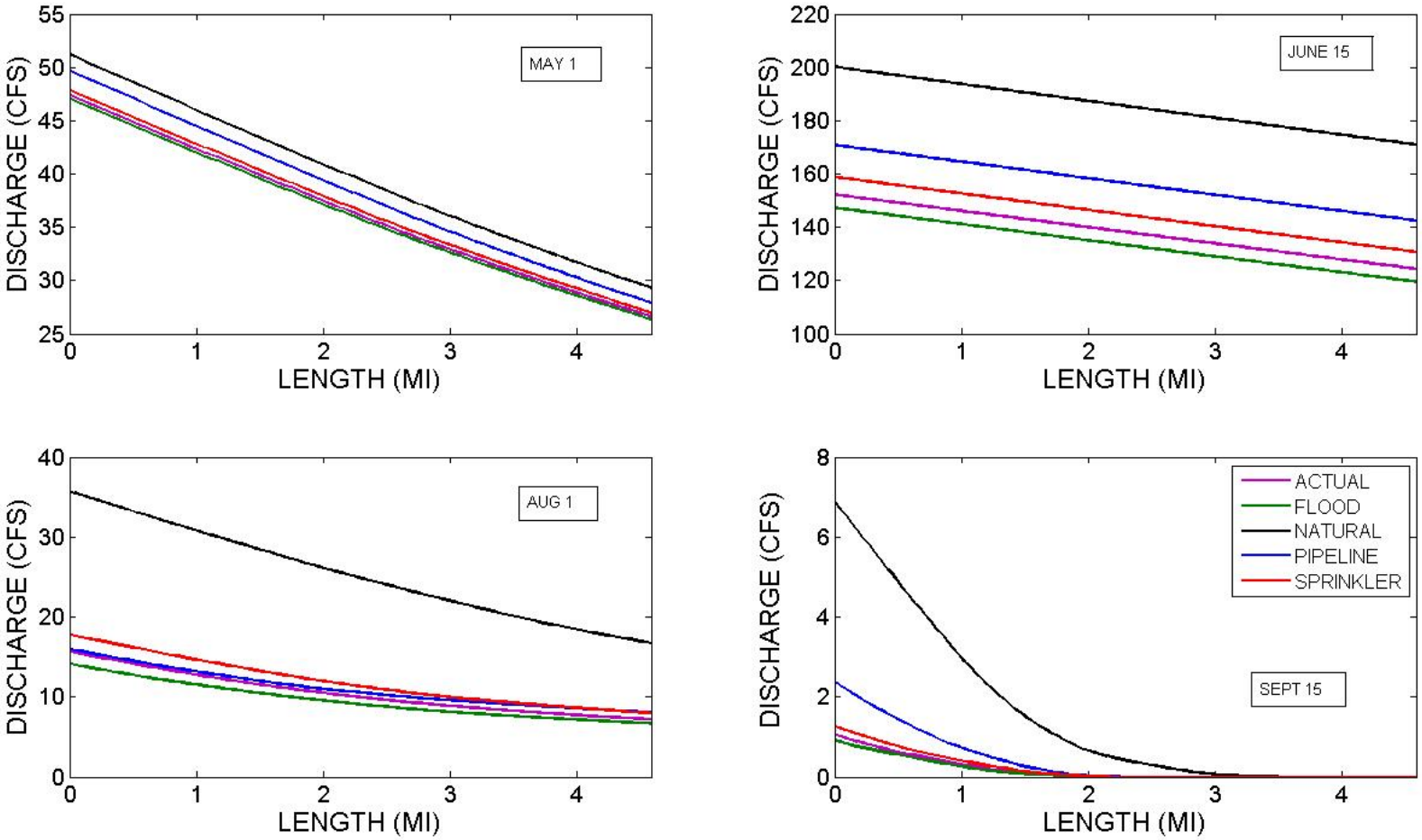

Figure 23: Mean discharge in North Leigh Creek versus distance across alluvial fan reach on the respective days.

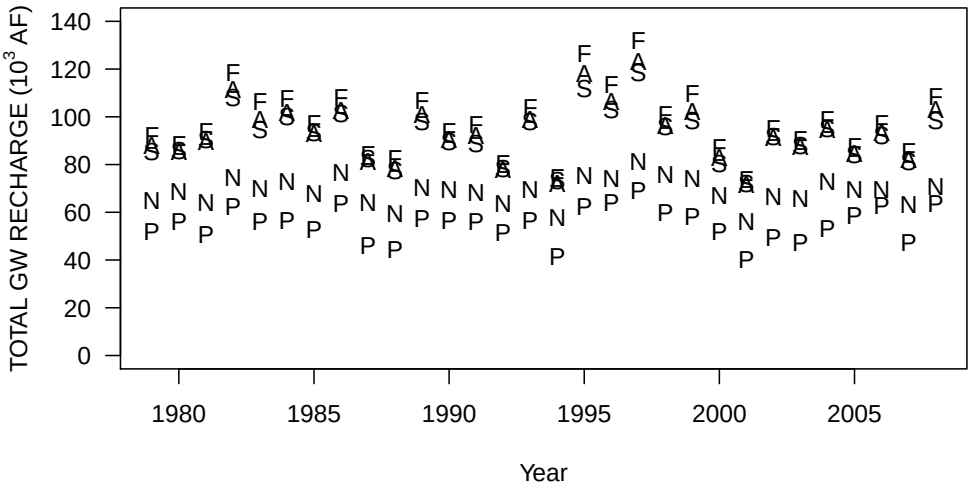

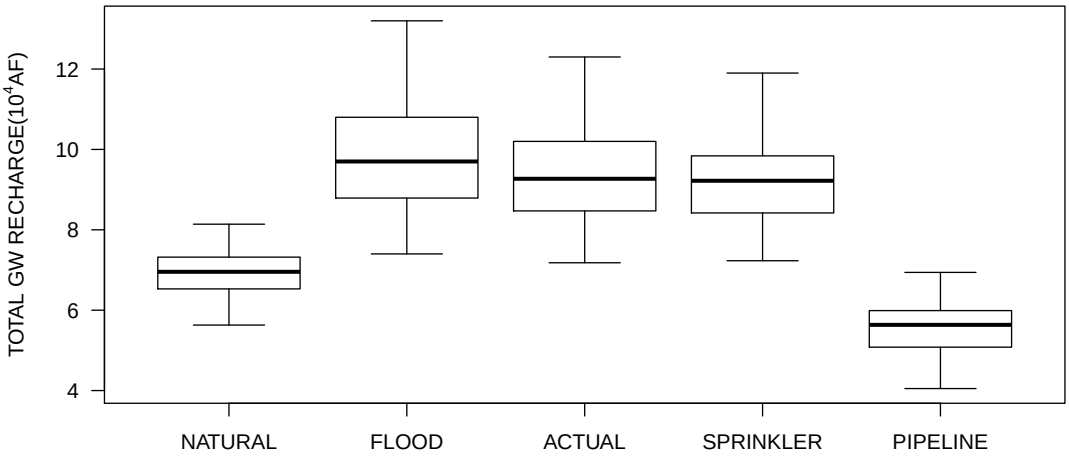

Figure 24: Total groundwater recharge by water year (top), and summarized over water years (bottom), by scenario. N = Natural, F = Flood, A = Actual, S = Sprinkler, P = Pipeline.

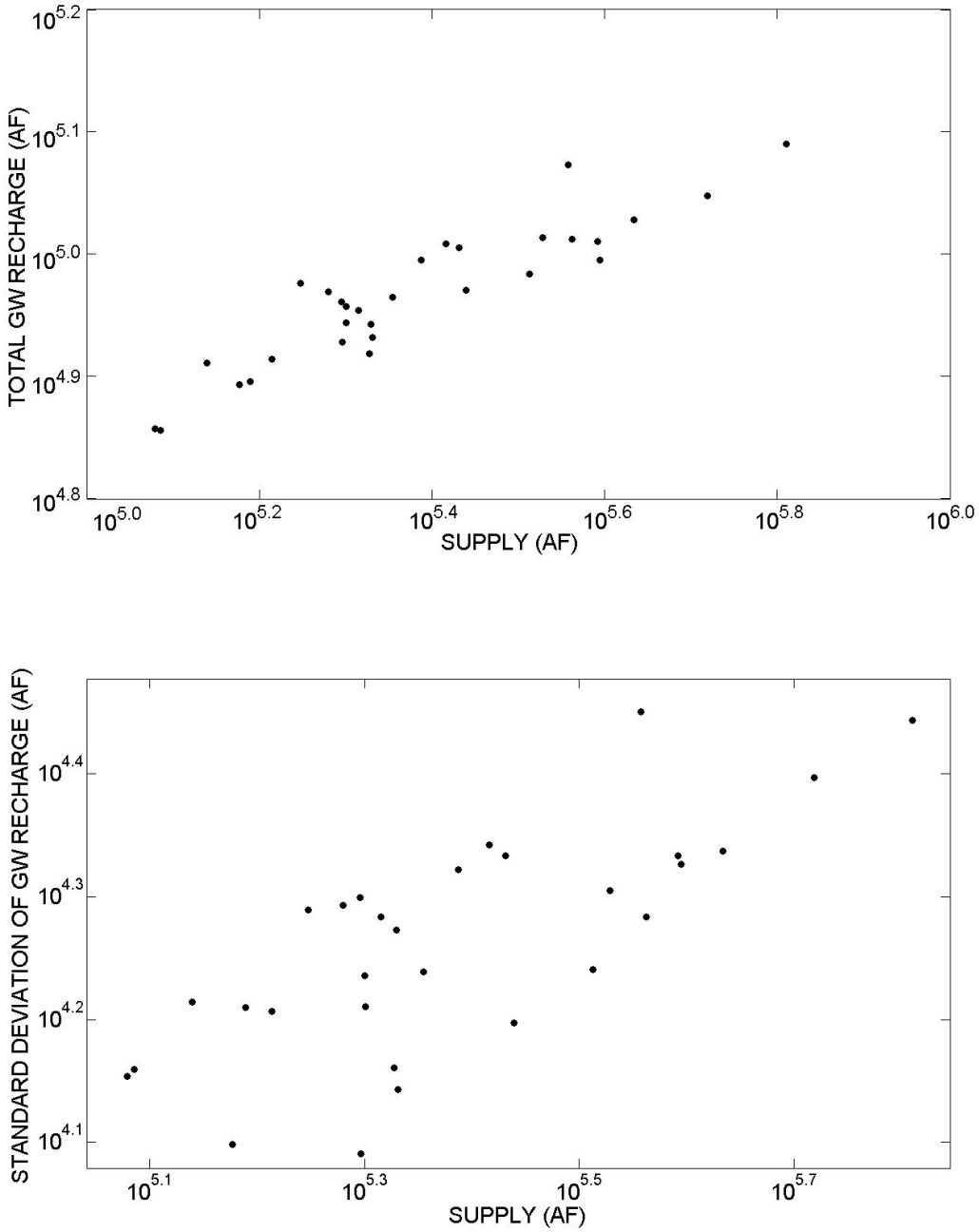

Figure 25: Total groundwater recharge under the actual scenario versus supply (top, log-log scale). Relationships for the other scenarios were similar (Table 5). Standard deviation in total groundwater recharge across scenarios versus supply (bottom, log-log scale).

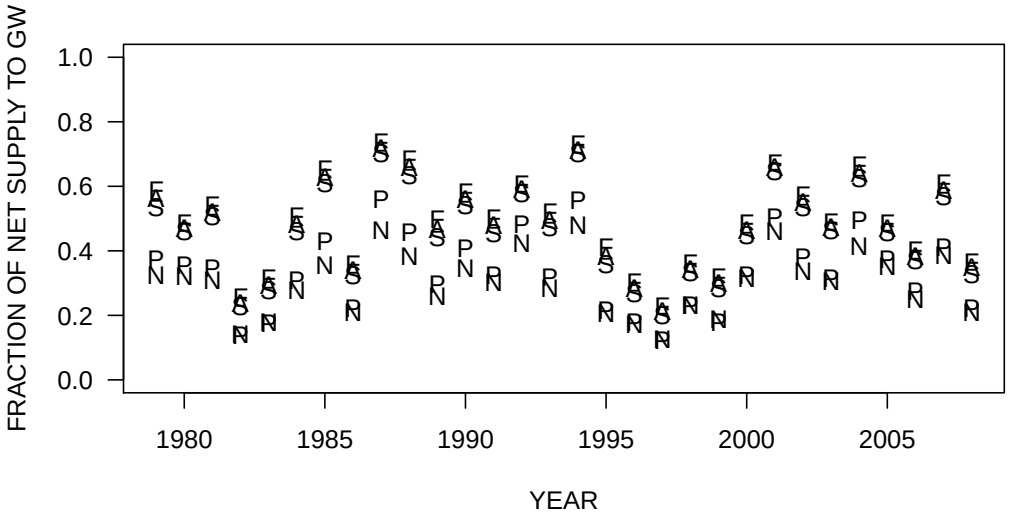

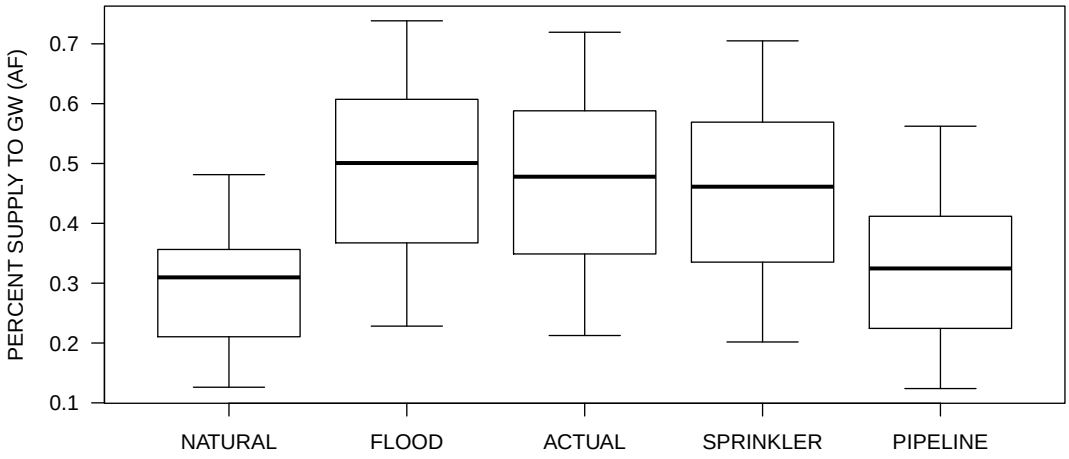

Figure 26: Percent of total groundwater recharge by water year (top), and summarized over water years (bottom), by scenario. N = Natural, F = Flood, A = Actual, S = Sprinkler, P = Pipeline.

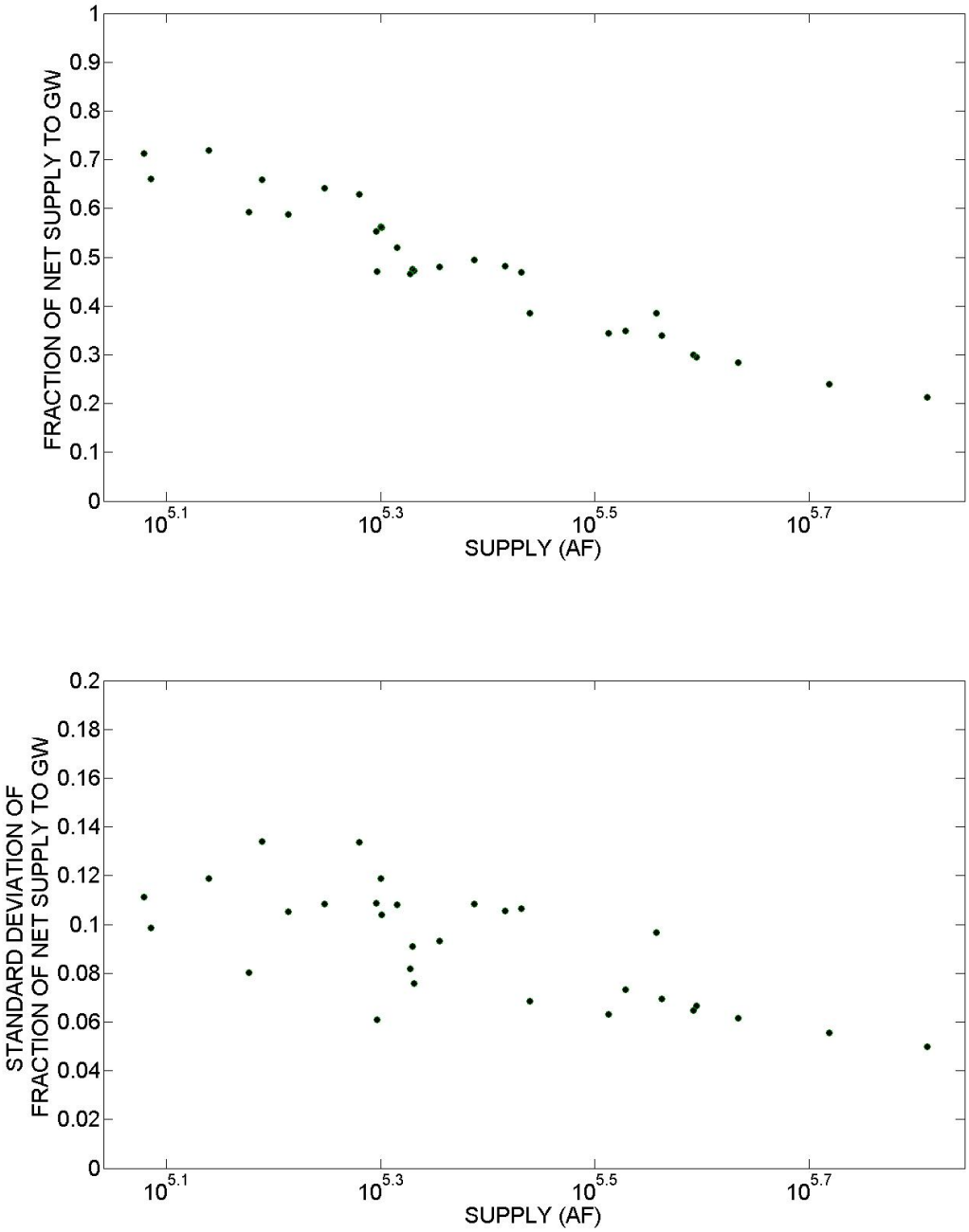

Figure 27: Percent of total groundwater recharge under the actual scenario versus supply (top). Relationships for the other scenarios were similar (Table 6). Standard deviation in percent of total groundwater recharge across scenarios versus supply (bottom).

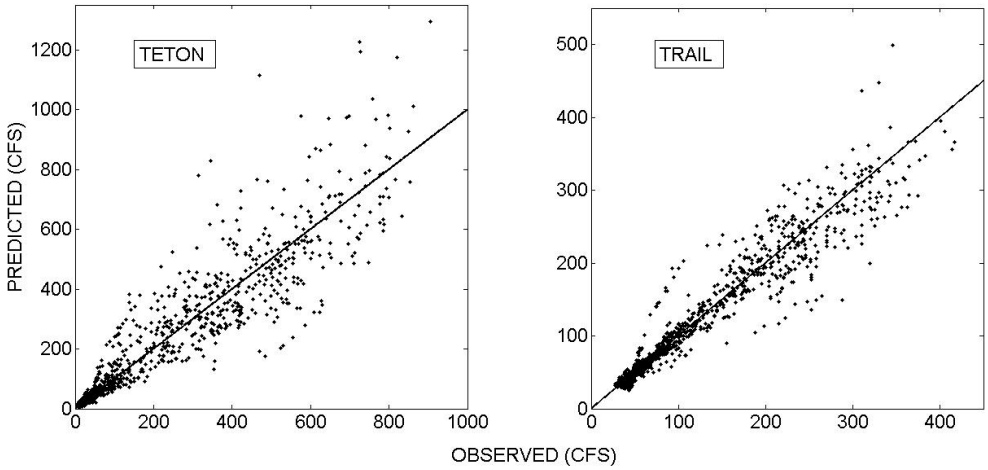

Figure 28: Model-predicted versus observed daily streamflow in Teton and Trail Creeks. Line is $y = x$.

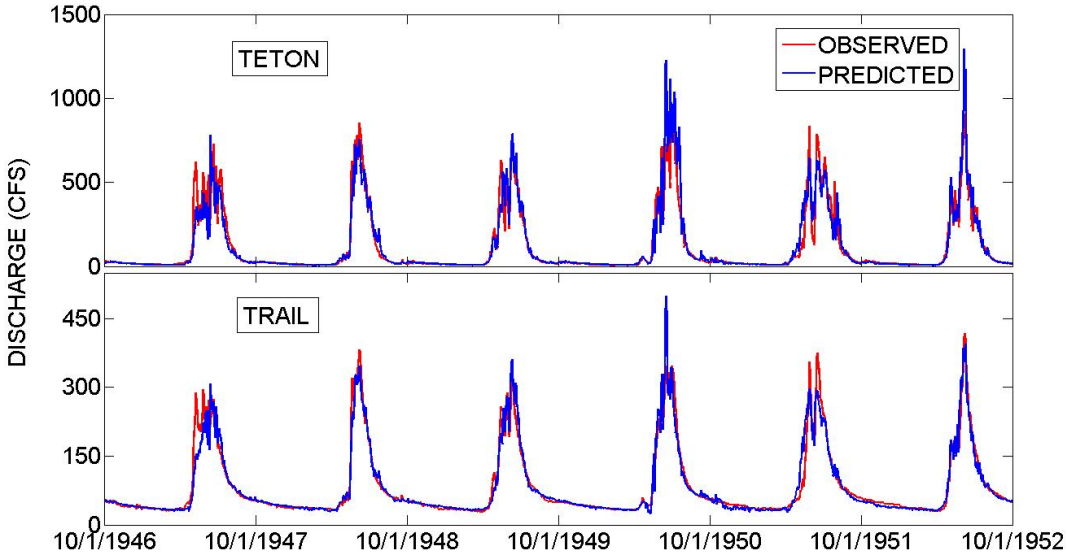

Figure 29: Model-predicted and observed Teton and Trail Creek hydrographs.

TABLES

Table 1: Basin parameters used in scaling Teton Creek streamflow to the other four creeks. Elevation information is given for reference. Data were gathered using the USGS streamstats application (http://streamstatsags.cr.usgs.gov).

Parameter	Teton	Darby	Fox	South Leigh	North Leigh
Basin Area (mi^2)	33.65	22.58	11.53	15.45	15.64
Mean Annual Precip (in)	52.80	53.40	53.00	50.80	49.70
Minimum Basin Elevation (ft)	6750	6460	6630	6910	6750
Maximum Basin Elevation (ft)	11400	11000	10900	10700	10500
Mean Basin Elevation (ft)	8890	8660	8580	8580	8300

Table 2: Loss rates (r) in the three channel types.

Channel Type	Mean estimate (ft/day)	Standard Error	n
Henry's Fork canals	2.655	0.4649	19
Teton Alluvial Fan Streams	3.397	0.7172	50
Teton Valley canals	3.663	0.9181	10

Table 3: Summary of Model Scenarios.

Scenario	Symbol	Diversion	Conveyance	Application
Natural	N	None	None	None
Flood	F	1.107 times actual	Historic (Table 4)	0% sprinkler
Actual	A	Actual rate	Current (Table 4)	Actual
Sprinkler	S	0.862 times actual	Current (Table 4)	90% sprinkler
Pipeline	P	Min(Crop ET, supply, capacity)	Pipes (0 seepage)	100% sprinkler (no loss))

Table 4: Lengths and areas for canal systems in the tributaries both historically and currently.

Stream	Historic Length (ft)	Current Length (ft)	Historic Area (ft^2)	Current Area (ft^2)
Trail Creek	107,030	78,788	920,977	682,801
Fox Creek	28,390	28,790	261,664	220,341
Darby Creek	54,659	40,251	575,960	437,383
Teton Creek	120,233	125,356	1,420,267	1,450,778
S. Leigh Creek	130,491	107,744	996,182	708,042
N. Leigh Creek	41,180	41,180	397,656	397,656
Total	481,983	422,109	4,572,706	3,897,001

Table 5: Linear Regression of logarithm of total groundwater recharge as a fraction of logarithm of water supply.

Scenario	Intercept	Slope	R^2	Adjusted R^2	P Value
Natural	9.000	0.173	0.747	0.738	7.67×10^{-10}
Flood	7.633	0.311	0.853	0.848	3.563×10^{-13}
Actual	7.887	0.286	0.839	0.833	1.281×10^{-12}
Sprinkler	8.312	0.251	0.795	0.788	3.733×10^{-11}
Pipeline	7.499	0.275	0.758	0.749	4.076×10^{-10}

Table 6: Linear Regression of logarithm of the percent of net supply moving through the aquifer as a function of logarithm of water supply.

Scenario	Intercept	Slope	R^2	Adjusted R^2	P Value
Natural	3.099	-0.226	0.964	0.963	2.2×10^{-16}
Flood	4.490	-0.322	0.916	0.913	2.2×10^{-16}
Actual	4.462	-0.322	0.926	0.923	2.2×10^{-16}
Sprinkler	4.443	-0.321	0.933	0.930	2.2×10^{-16}
Pipeline	3.790	-0.279	0.934	0.931	2.2×10^{-16}

Table 7: Measures of error at the daily scale for Teton Creek and Trail Creek streamflow prediction models.

Metric	Teton Creek	Trail Creek
Bias (cfs)	1.06	-1.01
Relative Bias	3.81%	-0.12%
Root Mean Square Error (cfs)	61.66	18.26
Mean Absolute Error (cfs)	25.37	8.77
Mean Relative Error	21.12%	9.07%
R^2	89.54%	94.27%
Nash-Sutcliffe Efficiency	88.74%	94.25%

Table 8: Results of model comparison for temporal conversion of irrigation methods to sprinkler application.

p_∞	$f(t)$	Degrees of freedom	$\triangle$AIC$_c$	AIC$_c$ weight	Evidence Ratio
0.9	$\log_e(t-1969)$	3	0	0.583	1
1.0	$\log_e(t-1969)$	3	0.173	0.412	1.4
1.0	t	3	2.600	0.003	181.2
0.9	t	3	2.872	0.003	312.2

Table 9: Results of model comparison for dependence of total diversion on total water supply and fraction p of irrigated land under sprinkler application.

$F(p)$	Degrees of Freedom	$\triangle$AIC$_c$	AIC$_c$ Weight	Evidence Ratio
$\frac{p}{1-p}$	4	0	0.49	1
0	3	1.86	0.19	2.54
$\log_e\left(\frac{p}{1-p}\right)$	4	2.43	0.14	3.37
p	4	3.06	0.11	4.62
$\log_e(p)$	4	3.80	0.07	6.69

APPENDIX A: THE DERIVATION OF THE DIFFUSION EQUATION FOR GROUNDWATER FLOW AND APPLICATION TO TETON VALLEY

Here, I outline the derivation of the standard Boussinesq equation for horizontal flow in an unconfined aquifer. An unconfined aquifer is in free communication with the atmosphere, that is, the top of the saturated zone is not fixed by geological constraints but is maintained in pressure equilibrium with the atmosphere (Hermance, 1999). Thus, the saturated thickness of the aquifer is not constant in either space or time. Define S_y to be specific yield, a dimensionless quantity describing the ratio of the volume of water released from the aquifer under gravity drainage to the volume of saturated aquifer. Conservation of mass in a volume element of the aquifer, combined with Darcy's Law, gives

$$\frac{\partial}{\partial t}\iiint S_y \, dV = \iiint \left[\nabla \cdot (K\nabla h) + R(x,y,z,t)\right] \, dV, \tag{17}$$

where R is the rate of recharge to the aquifer, if positive, or discharge, if negative, with dimension $\left[\frac{1}{T}\right]$. The equation as a whole has dimension $\left[\frac{L^3}{T}\right]$. Assuming a horizontal aquifer bottom at $z = 0$, applying Equation (17) to a vertical column of saturated aquifer of cross-sectional area A yields

$$\frac{\partial}{\partial t}\iint_A \int_0^{g(x,y,t)} S_y \, dz \, dA = \iint_A \int_0^{g(x,y,t)} \nabla \cdot (K\nabla h) + R(x,y,z,t) \, dz \, dA, \tag{18}$$

where $z = g(x,y,t)$ is the top of the saturated zone (water table). Because Equation (18) must hold for any arbitrary cross section,

$$\frac{\partial}{\partial t}\int_0^{g(x,y,t)} S_y \, dz = \int_0^{g(x,y,t)} \nabla \cdot (K\nabla h) + R(x,y,z,t) \, dz. \tag{19}$$

In order to evaluate the integrals, I make the so-called Dupuit assumption (Hermance,

1999), which applies to groundwater flow systems in which vertical gradients in h are negligible and flow is primarily horizontal. From Darcy's Law, the direction of flow and surfaces of constant hydraulic head h are always orthogonal. If the aquifer bottom is horizontal, the vertical component of flow at the aquifer bottom is zero, so level surfaces of h are oriented vertically at their intersection with the bottom. In general, the surface $z = g(x, y, t)$ defining the top of the saturated zone is not horizontal, so there is some vertical component of flow at the top of the saturated zone. However, if the gradient of $g(x, y, t)$ with respect to x and y is small, then $z = g(x, y, t)$ is nearly horizontal, and level surfaces of h are very nearly vertical at their intersection with $z = g(x, y, t)$. Thus, except near strong vertical gradients, such as those created by a pumping well, level surfaces of h are essentially vertical from the aquifer bottom to the top of the saturated zone, implying that 1) $\dfrac{\partial h}{\partial z} \approx 0$ (i.e., $h(x, y, z, t) \approx h(x, y, t)$), and 2) $g(x, y, t) \approx h(x, y, t)$. Making these substitutions in Equation (19) and integrating with respect to z yields

$$S_y \frac{\partial h}{\partial t} = \nabla \cdot (K \nabla h) + F(x, y, t), \tag{20}$$

where S_y and K now represent vertically averaged storativity and conductivity, respectively, and $F(x, y, t) = \int_0^h R(x, y, z, t)\, dz$ is specific rate of recharge $\left[\dfrac{L}{T}\right]$ at (x, y, t).

In the Teton Valley alluvial aquifer, the assumptions required for use of Equation (20) are met, at least on average. The bottom of the alluvial aquifer has roughly the same slope as the surrounding fault-block mountains (Figure 2), about 5000 vertical feet over 9 miles (10%). Thus, the aquifer bottom is close to horizontal. The elevation of the water table decreases about 250 feet from the tops of the alluvial fans to the point of discharge at the springs, a horizontal distance of about 5 miles (Figure 1). Thus, the gradient of the top of the saturated zone is less than one percent, so the Dupuit assumption is met.

If the aquifer is isotropic and homogeneous, meaning S_y does not depend on x and y and K is equal in all directions, then I obtain the Boussenesq equation for horizontal flow in an unconfined aquifer

$$S_y \frac{\partial h}{\partial t} = K \left[\frac{\partial}{\partial x} \left(h \frac{\partial h}{\partial x} \right) + \frac{\partial}{\partial y} \left(h \frac{\partial h}{\partial y} \right) \right] + F(x, y, t). \tag{21}$$

Equation (21) is nonlinear in h. However if changes in h are small relative to the mean saturated aquifer thickness, it can be linearized. In Teton valley, the hydraulic head has changed 20 to 30 feet out of several hundred feet of saturated thickness over the decades (Nicklin Earth and Water, Inc., 2003). The change on a year-to-year scale is approximately 50 to 60 feet out of several hundred (USGS well data). Therefore changes in h are small relative to mean saturated thickness, so the model for Teton valley may be linearized, leading to

$$\frac{\partial u}{\partial t} = \frac{K h_0}{S_y} \left[\frac{\partial^2 u}{\partial x^2} + \frac{\partial^2 u}{\partial y^2} \right] + \frac{F(x, y, t)}{S_y}, \tag{22}$$

where $u(x, y, t) = h(x, y, t) - h_0$, h_0 is mean saturated thickness. This flow model has a diffusion coefficient $\frac{K h_0}{S_y}$, which is the mean hydraulic diffusivity. Specific boundary and initial conditions accompany Equation (22).

In Teton Valley, Equation (22) can be applied on a model domain that is approximately rectangular with a length $L = 20$ miles and width $W = 5$ miles and extends from Trail Creek in the south to North Leigh Creek in the north (Figure 1). The origin of the coordinate system is at the southwest corner of the domain. This creates the boundaries of the domain: $x = 0$ (west), $y = 0$ (south), $x = W$ (east), and $y = L$ (north). It is assumed that the hydraulic head, h_0, is fixed at the groundwater spring discharge boundary $x = 0$. It is reasonable to assume that no water flows into or out of the domain as groundwater along the south, east, and north boundaries, and the only source of inflow to the aquifer is due to

recharge (Van Kirk and Jenkins, 2005). These assumptions produce the following boundary conditions for Equation (2):

$$\begin{aligned}
u(0,y,t) &= 0 \text{ for } 0 \leq y \leq L \text{ and } t > 0 \\
\frac{\partial u}{\partial y}(x,0,t) &= 0 \text{ for } 0 \leq x \leq W \text{ and } t > 0 \\
\frac{\partial u}{\partial x}(W,y,t) &= 0 \text{ for } 0 \leq y \leq L \text{ and } t > 0 \\
\frac{\partial u}{\partial y}(x,L,t) &= 0 \text{ for } 0 \leq x \leq W \text{ and } t > 0.
\end{aligned}$$

For any given modeling scenario, the initial condition for the groundwater model should be the state of the system that would have existed under that scenario at the beginning of the model time frame, i.e., at the beginning of water year 1979. This condition is unknown, but we can simulate an approximation to it by initiating the groundwater model with zero hydraulic gradient ($u(x,y,0) = 0$ for all x and y) and solving forward in time using a recharge function $F(x,y,t)$ that represents the mean recharge for that particular scenario. This recharge function will be periodic in time with period one year, so the model state will converge to a periodic solution with period one year. The value of this solution at the beginning of the water year then represents the mean distribution of hydraulic head under that scenario at the beginning of the water year and thus is a reasonable approximation to the desired initial condition.

The only streamflow gage in the model domain is located near the northern boundary, where the majority of aquifer discharge has returned to the river via springs. Therefore, I need only calculate total discharge from the aquifer and not the spatial distribution of discharge along the springs. Thus I can reduce the model to one spatial dimension by averaging across the aquifer length. This is accomplished by dividing Equation (22) by L

and integrating with respect to y from 0 to L, that is,

$$\frac{\partial}{\partial t}\frac{1}{L}\int_0^L u(x,y,t)\,dy = \frac{Kh_0}{S_y}\left[\frac{\partial^2}{\partial x^2}\frac{1}{L}\int_0^L u(x,y,t)\,dy + \frac{1}{L}\frac{\partial u}{\partial y}\bigg|_0^L\right] + \frac{1}{L}\int_0^L \frac{F(x,y,t)}{S_y}\,dy. \tag{23}$$

Applying the no flux boundary conditions at $y = 0$ and $y = L$, letting $D = \dfrac{Kh_0}{S_y}$, defining $p(x,t) = \dfrac{1}{L}\int_0^L u(x,y,t)\,dy$ and $C(x,t) = \dfrac{1}{L}\int_0^L F(x,y,t)\,dy$, I obtain

$$\frac{\partial p}{\partial t} = D\frac{\partial^2 p}{\partial x^2} + \frac{1}{S_y}C(x,t), \tag{24}$$

with boundary conditions $p(0,t) = \dfrac{\partial p}{\partial x}(W,t) = 0$ for $t > 0$.

Recall that total discharge across a surface Ω was given by Equation (3). If Ω is a vertical plane at $x = 0$, then the total discharge out of the aquifer is

$$\begin{aligned} Q(t) &= -\int_0^L Kh_0\frac{\partial h}{\partial x}\bigg|_{x=0} dy(-1) \\ &= Kh_0\int_0^L \frac{\partial u}{\partial x}\,dy \\ &= Kh_0 L\frac{\partial p}{\partial x}\bigg|_{x=0}. \end{aligned} \tag{25}$$

This represents the contribution of aquifer discharge to streamflow in the Teton River at the gage located near the northern boundary of Teton valley.

APPENDIX B: STREAMFLOW SYNTHESIS VALIDATION

A jacknife procedure was used to validate the streamflow synthesis model. The model was fit to five of the six years for which data were available. This model was used to predict streamflow over the sixth year. This process was repeated, removing a different year each time, until all six years had been predicted from models fit to the other five. This resulted in predicted streamflow from water years 1947 to 1952, which could be compared to actual data during the same time period.

The following error measures were used for model validation:

$$\text{Bias} = \frac{1}{n}\sum_{i=1}^{n}(\widehat{Q_i} - Q_i)$$

$$\text{Relative Bias} = \frac{1}{n}\sum_{i=1}^{n}\frac{(\widehat{Q_i} - Q_i)}{Q_i}$$

$$\text{Root Mean Square Error} = \sqrt{\frac{\sum_{i=1}^{n}(\widehat{Q_i} - Q_i)^2}{n}}$$

$$\text{Mean Absolute Error} = \frac{1}{n}\sum_{i=1}^{n} \mid \widehat{Q_i} - Q_i \mid$$

$$\text{Mean Relative Error} = \frac{1}{n}\sum_{i=1}^{n}\frac{\mid \widehat{Q_i} - Q_i \mid}{Q_i}$$

$$\text{R}^2 = [cor(\widehat{Q_i}, Q_i)]^2$$

$$\text{Nash-Sutcliffe Modeling Efficiency} = 1 - \frac{\sum_{i=1}^{n}(\widehat{Q_i} - Q_i)^2}{\sum_{i=1}^{n}(Q_i - \overline{Q})^2}$$

where $\widehat{Q_i}$ is the predicted value on day i, Q_i is the observed value on day i , $\overline{Q}$ is the mean of Q_i, and n is the number of days modeled (2190). The results of these error estimates for Teton Creek and Trail Creek are summarized in Figures 28 and 29, and Table 7.

APPENDIX C: DESCRIPTIVE MODEL OF IRRIGATION CONVERSION RATE

Four candidate models were proposed of the form

$$p(t) = \frac{p_\infty}{1 + \exp(-a - bf(t) - \epsilon)}, \tag{26}$$

where $p(t)$ is the fraction of irrigated land under sprinkler irrigation in year y, p_∞ is the fraction of irrigated land that will ultimately be irrigated with sprinklers, $f(t)$ is a strictly increasing function of year t, a and b are coefficients to be estimated statistically ($b > 0$ for the case in which $p(t)$ increases with t), and ϵ is a random, normally distributed error variable with mean zero. In general, Equation (26) describes a sigmoidal dependence of p on t in which $p(t) \to 0$ for t sufficiently small and $p(t) \to p_\infty$ as t becomes large. Equation (26) is algebraically equivalent to

$$\ln\left(\frac{p(t)}{p_\infty - p(t)}\right) = a + bf(t) + \epsilon, \tag{27}$$

so that the statistical estimation can be performed by linear regression of $\ln\left(\frac{p(t)}{p_\infty - p(t)}\right)$ versus $f(t)$, which yields unbiased coefficient estimates and diagnostic statistics provided that the residuals ϵ are normally distributed.

I proposed four candidate models of the general form given by Equation (26), fit each using Equation (27), and used Akaike's Information Criterion with small sample correction (AIC_c) to rank the models (Burnham and Anderson, 2002). The four models consisted were defined by specifying two choices for each of p_∞ and $f(t)$. The choices for p_∞ were 1, under the assumption that eventually all irrigated land will be irrigated with sprinklers, and 0.9, based on the observation of Contor (2004) that the conversion rate slowed dramatically after the early 1990s and field observations indicating that currently about 90%

of the irrigated land in the Henry's Fork watershed is under sprinkler irrigation. The two choices for $f(t)$ were $f(t) = t$ and $f(t) = \ln(t - 1969)$. When $f(t) = t$, Equation (26) is a logistic function in which $p(t) \to 0$ only the limit as $t \to -\infty$. When $f(t) = \ln(t - 1969)$, Equation (26) becomes a rational function in t in which $p(t) = 0$ in the year 1969. I chose 1969 because the earliest irrigation method conversion project in the study area of which I am aware was the conversion of the Trail Creek irrigation system from a traditional canal-and-flood system to a pipeline-and-sprinkler system. This project began in the late 1960s and was completed by the early 1970s. Proposal of these four models allowed me to use the standard logistic function as a "null" model to which to compare the hypotheses that conversion to sprinklers began no earlier than 1969 and that the fraction of land under sprinkler irrigation has leveled off in recent years to its current value of about 90%. Use of my knowledge of the initial and current states of the conversion process to propose models is consistent with the framework described in Burnham and Anderson (2002) for use of information-theoretic model selection.

The AIC_c analysis showed that there was essentially no evidence from the data that conversion to sprinkler irrigation commenced prior to 1969 (Table 8). Among the two models in which $f(t) = \ln(t - 1969)$, the data provided somewhat more evidence for the model with $p_\infty = 0.9$ than for the model with $p_\infty = 1$, suggesting that fraction of land in sprinkler irrigation has approached its long-term and current value of around 90%. Thus, I chose as our "best" descriptive model of conversion from surface to sprinkler application methods the equation

$$p(t) = \frac{0.9}{1 + \exp(8.52 - 3.31\ln(t - 1969))} = \frac{0.9(t - 1969)^{3.31}}{(t - 1969)^{3.31} + 5014}, \tag{28}$$

where t is in years (Figure 4). Adjusted R^2 for this model was 87.5%. A normal probability

plot showed that the residuals from this model were normally distributed.

APPENDIX D: ESTIMATION OF CANAL LENGTHS AND WIDTHS

To estimate canal widths and lengths, I first determined the extent of the current canal system through a combination of field reconnaissance and analysis of Google Earth images and 7.5-minute topographic maps. I used Google Earth's length measurement tool to measure the total length of each individual canal system that diverts water from each of the six model streams. The number of individual canals on each stream ranged from four to nine. I then randomly selected 10 points on each of these canals and measured canal width at each of these points using Google Earth's measurement tool (40 to 90 width measurement points for each of the six streams). For many canals, I had actual width measurements from field observations, in which case I used the field observation as one measurement and randomly selected nine other locations for measurement using Google Earth. Although linear features such as canals are easily identifiable on Google Earth satellite images, the width of these features is small relative to image resolution, so I developed an empirical model to correct widths measured on Google Earth images for bias. I randomly selected 20 locations in areas of the Henry's Fork watershed served by canals and visited the point nearest each selected location at which a public road crossed a canal. I measured the width of the canal water surface at each of these road crossings during the peak of irrigation season and measured the apparent width of the canal water surface at these same locations on Google Earth images that were taken during the peak of irrigation season. I then fit to these true (field-measured) and Google Earth-measured widths a regression model of the form $\ln(Truewidth) = a + b * \ln(GoogleEarthwidth) + \epsilon$, where ϵ is a normally distributed, random error variable. This relationship describes a power function that was used to correct image-estimated widths for bias. Using feet as measurement units, the regression parameters were $a = 1.126$ and $b = 0.669$. Model R^2 was 71.5%, and residuals met distributional

assumptions. The model indicated that measurements of canal width using Google Earth overestimated width when image-measured width was less than 30 feet and underestimated widths when image-measured width was greater than 30 feet.

I averaged the 10 width measurements to obtain a single mean width for each canal system. Multiplication of mean width by total length produced the estimated area of each canal system. Summing these over all canal systems served by a given stream gave total wetted area of the canal systems served by that stream (Table 4). A similar procedure was followed to estimate areas of riparian vegetation along streams and canals.

APPENDIX E: ESTIMATION OF DIVERSION RATES UNDER FLOOD AND SPRINKLER SCENARIOS

I first developed a statistical model that predicted how diversion rate changed as a function of fraction of irrigated land under sprinkler application. Because the ET analysis was performed at the scale of the entire model domain rather than at the individual stream scale, I performed the analysis of diversion versus application method over the entire domain. Thus, I used total annual diversion over the six streams as the response variable, estimated fraction of irrigated land under sprinkler irrigation in a given year (Section 3.2.2, Figure 4) as the predictor variable, and total annual water supply (sum of water-year discharge over the six model streams) as a covariate, the effect of which was removed prior to computing the effect of irrigation method. To account for large interannual variability in total diversion and total supply, I used ln-transformed values of these variables in the analysis. I again used an information-theoretic approach to model selection, proposing and comparing five different models of the form

$$\ln(Diversion(t)) = \alpha + \beta_1 \ln(Supply(t)) + \beta_2 F(p(t)) + \epsilon, \tag{29}$$

where $Diversion(t)$ is total diversion for the six streams in water year t, $Supply(t)$ is the total inflow for the six streams in water year t, $p(t)$ is estimated fraction of irrigated land under sprinkler application in year t, F is one of five different possible transformations of $p(t)$, and ϵ is a random, normally distributed error variable. The five functional forms for F were the zero function (no dependence on sprinkler irrigation fraction; this served as a null model), the identity function, the natural logarithm, the odds $F(p) = p/(1-p)$, and the logit $F(p) = \ln(p/(1-p))$ (Table 9).

The model in which $F(p) = p/(1-p)$ was most strongly weighted (Table 9) and

was over 2.5 times more likely to have resulted from the given data than any of the other candidate models, including the null model (no dependence on irrigation method). Residual analysis showed that the residuals were normally distributed, displayed constant variance across fitted values, and were temporally independent. Hence, I took this model to be the best description of the dependence of diversion rate on sprinkler application fraction, after accounting for water supply. The predictive model, in units of acre-feet, was

$$Diversion(t) = 76.62 \cdot Supply(t)^{0.577} \cdot \exp\left(-0.027\frac{p}{1-p}\right) \tag{30}$$

Thus, at a given water year supply, diversion was a decreasing function of $p/(1-p)$, which can be interpreted as the odds that a given irrigated parcel of land was under sprinkler irrigation in that year. This model accounted for 73.5% of the observed variability in ln-transformed annual diversion; dependence on water supply accounted for 69.2% of the variability, and dependence on fraction of irrigated land under sprinkler application accounted for the remaining 4.3%.

Equation (30) was then used to predict the total diversion for each water year in the modeling period under flood irrigation ($p = 0$) and current conditions (90% sprinkler, $p = 0.9$). However, this model was developed for all six streams and whole water years. To downscale the model to be applicable to individual streams on individual days of the water year, it was assumed that the actual irrigation-season diversion hydrograph for a particular stream in a particular water year could be scaled by a proportionality constant to obtain the irrigation-season diversion hydrograph for that water year under the flood and sprinkler scenarios. This proportionality constant would then be the same at both the annual and daily scales. Because the irrigation scenarios are hypothetical and hence the diversion rate under a given scenario was not known for an individual water year, I computed the proportionality

constant as the ratio of the predicted diversion rate under the flood or sprinkler irrigation scenario and the predicted diversion under the actual scenario, where Equation (30) was used to compute these predicted values, and Equation (26) was used to compute the value of p under the actual scenario. These ratios were estimated with linear regression in which the intercept was forced to be 0.

Linear regression of predicted diversion under the sprinkler scenario with that predicted under the actual scenario showed the intercept was not significantly different from 0 ($t_{28} = 1.458$, $P = 0.156$), confirming that the ratio model was appropriate. After forcing the intercept to be 0, the ratio of diversion under the sprinkler irrigation scenario to that under the actual scenario was 0.862, and this model accounted for 99.6% of the variability in predicted sprinkler-scenario diversion. Residuals met assumptions of the linear regression. Thus, on any day of any water year on any given stream, the predicted diversion rate under the sprinkler irrigation scenario was 86.2% of that observed under the actual scenario. The ratio of predicted flood-scenario diversion to predicted actual diversion was 1.107; statistics were identical to that for the sprinkler scenario.